TECHNICAL REPORT STANDARD PAGE

1. Report No.	2. Government Accession No.	3. Recipient's Catalog No.
FHWA/LA.06/409		

4. Title and Subtitle	5. Report Date
Evaluation of Stone/RAP Interlayers Under Accelerated Loading	April 2007
	6. Performing Organization Code LTRC

7. Author(s)	8. Performing Organization Report No.
Louay N. Mohammad, Ph.D.; Masood Rasoulian, P.E.; Bill King, P. E.; Mark Martinez; and Yan Qi	LTRC Project No. 00-1P State Project No. 736-99-1023

9. Performing Organization Name and Address	10. Work Unit No.
Louisiana Transportation Research Center 4101 Gourrier Avenue Baton Rouge, LA 70808	11. Contract or Grant No.

12. Sponsoring Agency Name and Address	13. Type of Report and Period Covered
Louisiana Transportation Research Center 4101 Gourrier Avenue Baton Rouge, LA 70808	Final Report July 1999-June 2005
	14. Sponsoring Agency Code LTRC

15. Supplementary Notes

16. Abstract

A common method used by the Louisiana Department of Transportation and Development (LADOTD) for pavement design of non-interstate highways is to lime treat the subgrade and place a stabilized layer of soil cement over it followed by a layer of hot mix asphalt. One consistent problem with this method of construction is the appearance of reflection cracking in the asphalt layer. This is due to naturally-occurring shrinkage cracking in the soil cement, which propagates upward through the asphalt layer and then forms a combination of transverse and block cracking. As the pavement ages, the cracks accelerate the deterioration of the pavement structure. The results of the first ALF experiment indicated that placing a crushed stone layer either on top of the cement stabilized layer or beneath the asphalt layer would increase the pavement load carrying capacity by five fold when compared to conventional pavement structures with only soil cement base course layer. This concept is generally known as stone interlayer or inverted pavement design. This experiment sought to evaluate alternative materials such as reclaimed asphaltic pavement (RAP) to make the stone interlayer system more economical. Hot mix asphalt pavements built on equivalent thicknesses (3.5 inches) of RAP and crushed limestone base courses built on top of 6 inches of soil layer stabilized with 10 percent cement were evaluated side by side under the accelerated traffic loading test. A third test lane also evaluated the performance of RAP placed on a thicker (10 inch) but weaker cement (5 percent) treated layer. The test results showed that the crushed stone and RAP had very similar pavement performance under accelerated loading. Therefore, the researchers concluded the RAP is a suitable alternative for crushed stone in a stone interlayer system. They also found that in a stone interlayer system, thicker layers of cement treated layers with lower cement content performed better than thinner soil stabilized layers.

17. Key Words	18. Distribution Statement
Accelerated Pavement testing, Asphalt, Interlayers, RAP, Stone, FWD, Dynaflect	Unrestricted. This document is available through the National Technical Information Service, Springfield, VA 21161.

19. Security Classif. (of this report)	20. Security Classif. (of this page)	21. No. of Pages	22. Price
N/A	None	85	N/A

Project Review Committee

Each research project has an advisory committee appointed by the LTRC director. The Project Review Committee (PRC) is responsible for assisting the LTRC administrator or manager in the development of acceptable research problem statements, requests for proposals, review of research proposals, oversight of approved research projects, and implementation of findings.

LTRC appreciates the dedication of the following Project Review Committee members in guiding this research study to fruition.

LTRC Administrator

Zhongjie "Doc" Zhang, Ph.D., P.E.
Pavement and Geotechnical Research Administrator

Members

Rick Holm	Zhong Wu
Phil Arena	Mike Boudreaux
Freddy Roberts	Kim Garlington
Don Weathers	John Metcalf
Craig Duos	Luanna Cambas
Mark Stinson	Neal West

Directorate Implementation Sponsor

William Temple, P.E.
DOTD Chief Engineer

Evaluation of Stone/RAP Interlayers Under Accelerated Loading

by

Louay N. Mohammad, Ph.D.
Professor of Civil and Environmental Engineering
Director, Engineering Materials Characterization Research Facility
Louisiana Transportation Research Center

Masood Rasoulian, P.E.
Senior Pavement Research Engineer

Bill King, P.E.
Pavement Research Facility Manager

Mark Martinez
Pavement Research E.I.

Yan Qi
Graduate Student, Louisiana State University

LTRC Project No. 00-1P
State Project No. 736-99-1023

conducted for

Louisiana Department of Transportation and Development
Louisiana Transportation Research Center

August 2008

ABSTRACT

A common method used by the Louisiana Department of Transportation and Development (LADOTD) for pavement design of non-interstate highways is to lime treat the sub-grade and place a stabilized layer of soil cement over it followed by a layer of hot mix asphalt. One consistent problem with this method of construction is the appearance of reflection cracking in the asphalt layer. This is due to naturally-occurring shrinkage cracking in the soil cement, which propagates upward through the asphalt layer and then forms a combination of transverse and block cracking. As the pavement ages, these cracks accelerate the deterioration of the pavement structure. The results of the first ALF experiment indicated that placing a crushed stone layer either on top of the cement stabilized layer or beneath the asphalt layer would increase the pavement load carrying capacity by five fold when compared to conventional pavement structures with only soil cement base course layer. This concept is generally known as stone interlayer or inverted pavement design.

This experiment sought to evaluate alternative materials such as reclaimed asphaltic pavement (RAP) to make the stone interlayer system more economical. Hot mix asphalt pavements built on equivalent thicknesses (3.5 inches) of RAP and crushed limestone base courses built on top of 6 inches of soil layer stabilized with 10 percent cement by volume were evaluated side by side under the accelerated traffic loading test. A third test lane also evaluated the performance of RAP placed on a thicker (10 inch) but weaker cement (5 percent by volume) treated layer.

The test results showed that the crushed stone and RAP had very similar pavement performance under accelerated loading. Therefore, the researchers concluded the RAP is a suitable alternative for crushed stone in a stone interlayer system. They also found that in a stone interlayer system, thicker layers of cement treated layers with lower cement content performed better than thinner soil stabilized layers.

ACKNOWLEDGMENTS

The U.S. Department of Transportation, Federal Highway Administration (FHWA), the Louisiana Department of Transportation and Development (LADOTD), and the Louisiana Transportation Research Center (LTRC) financially support this research project. The assistance of the pavement research facility and the asphalt laboratory staff at LTRC is greatly appreciated. The guidance of the Project Review Committee to this research project is acknowledged.

IMPLEMENTATION STATEMENT

This project successfully demonstrated that RAP materials could be used as an alternative to stone interlayer in construction of the pavement base layers in Louisiana. Currently, several projects use RAP as an interlayer. The results of this experiment have been planned for implementation in the rehabilitation of a pavement structure of LA 103 in St. Landry Parish. RAP has been used as an interlayer in an HMAC overlay project in US 190, near Lotti. Recommendations are being made for further implementation of RAP use in pavement construction, in addition to further research at the PRF facilities (RAP in ALF 4 stabilized as stone alternative).

TABLE OF CONTENTS

LIST OF TABLES

LIST OF FIGURES

INTRODUCTION

The first experiment, Evaluation of Louisiana's Conventional and Alternative Base Courses, showed that pavement performance could be enhanced significantly if a layer of stone were placed over the cement stabilized subgrade and below the flexible HMAC layer. The concept is referred to as "stone interlayer design." The increase in performance level could be attributed to strengthening the area between the soil cement and the flexible layer and providing a medium for moisture discharge. Although the stone interlayer could not be effectively evaluated in an accelerated test, the stone interlayer should reduce the reflective soil cement shrinkage cracking.

LADOTD is in possession of large quantities of reclaimed asphaltic pavement (RAP) produced from various rehabilitation jobs throughout the state. RAP is asphalt concrete material removed and/or reprocessed from pavements undergoing reconstruction or resurfacing. Asphalt pavement is generally removed either through milling or full-depth removal. Milling entails removal of the pavement surface using a milling machine, which can remove up to a two-inch thickness in a single pass. Full-depth removal involves ripping and breaking the pavement using a rhino horn on a bulldozer and/or pneumatic pavement breakers. In most instances, the broken material is picked up and loaded into haul trucks by a front-end loader and transported to a central facility for processing. At this facility, the RAP is processed using a series of operations, including crushing, screening, conveying, and stacking. Nationwide, it has been estimated that as much as 80 to 85 percent of the excess asphalt concrete presently generated is being used either as a portion of recycled hot mix asphalt, in cold mixes, or as aggregate in granular or stabilized base materials.

LADOTD has an estimated 258,000 plus cubic yards of RAP in stockpile, with an annual accumulation of 468,000 cubic yards from implementation of the overlay program. This is equivalent to 50 percent of the total RAP produced. The other 50 percent is given as a cost reduction incentive to the contractors. At a cost of $15.00 per cubic yard, total utilization of this material in construction of an interlayer would save the state over $7 million annually in addition to improving the life expectancy of roadway pavements.

Currently, LADOTD allows the incorporation of RAP into asphalt mixes for pavement construction. The amount of RAP allowed is 30 percent RAP (by weight of the total mix) in base courses, 20 percent in binder courses, and 30 percent in flexible base courses. RAP is mixed with virgin aggregate and asphalt as needed, then placed. However, in this project, RAP was used in its raw form (100 percent RAP), without any rejuvenating or stabilizing agents, as an alternate replacement of an aggregate base layer. This was done to answer

several concerns regarding cost savings as well as pavement performance. The potential for improved pavement life using the RAP base materials in lieu of the stone base was investigated in this project.

The performance of the RAP base materials in the stone interlayer pavement design will be compared to that of the stone in the interlayer design. Additionally, a thicker treated subgrade section with reduced cement (5 percent by volume) will be compared to the thinner stabilized subgrade with standard cement (10 percent by volume), both having the interlayer RAP base materials.

OBJECTIVE

The primary objective of this study was to determine the effectiveness of using an untreated RAP interlayer in lieu of stone interlayer in a soil-cement asphalt pavement structure under accelerated loading. The secondary objective was to investigate the performance of soil cement sub-base courses by varying layer thickness and cement content.

SCOPE

Three asphalt pavement test lanes were constructed with different interlayer and soil cement sub-base courses. Each lane had a similar HMA top layer paved in two courses: 38 mm conventional Louisiana Type 8F wearing course and 51 mm Type 8F binder course. The interlayers and sub-bases for Lanes 1, 2, and 3 were: 89 mm untreated RAP and 254 mm, 5 percent cement stabilized soil; 89 mm untreated RAP and 152 mm, 10 percent cement stabilized soil; and 89 mm crushed stone and 152 mm, 10 percent cement stabilized soil, respectively. All three lanes had silty clay embankment. Lanes 1 and 2 had different soil cement sub-base courses, whereas, Lanes 2 and 3 had different interlayer courses.

Each test lane was loaded using Louisiana's Accelerated Loading Facility (ALF). Falling Weight Deflectometer (FWD) and DYNAFLECT tests were conducted on each test lane at every 25,000 ALF loading passes. Rutting and surface cracking were periodically measured. In addition, a suite of laboratory materials characterization tests was performed. The asphalt mixture tests included indirect tensile strength, indirect tensile resilient modulus, indirect tensile and axial creep test, and repeated shear at constant height test. Furthermore, repeated load triaxial tests were performed on the base course materials.

METHODOLOGY

Site Layout and Test Lane Construction

Figure 1 illustrates the layout design and cross section, respectively, of each of the three test lanes constructed for this study. Lane 1 was designed for 3½" RAP base over 10 inches of cement treated subgrade with 5 percent cement content (by volume). Lane 2 was designed for 3½" RAP base over 6 inches of cement stabilized subgrade with 10 percent cement content (by volume). Lane 3 was designed for 3½" stone base over 6 inches of cement stabilized subgrade with 10 percent cement content (by volume). A-4 soil was used for grade adjustments within the selected test lanes.

The Louisiana Department of Transportation and Development (LADOTD) uses two types of soil cement base course designs: cement stabilized design and cement treated design. Cement stabilized design (CSD) is governed by one of four methods, as described in LADOTD Test Method TR 432-02 [9]. The current practice in the CSD is to determine the percentage of cement that produces a minimum unconfined compressive strength of 300 psi at seven days curing for soil aggregate or recycled bases. Cement treated design (CTD) refers to materials blended with low cement content (four to six percent by volume) and has a minimum seven day unconfined compression strength of 150 psi.

A 2" binder course and 1½"wearing course HMAC was placed on top of each test lane. Also included in the design was the installation of a perforated drain pipe system located at the edge of each test lane. Each lane was constructed on an existing 5' embankment.

The conventional mix design consisted of Type 8 binder course with PAC-40 asphalt cement and a Type 8 Wearing Course with PAC-40 asphalt cement. Louisiana Type 8 mixtures are designed for high speed, high volume pavements that require the use of modified asphalt.

The contract was awarded to F.G. Sullivan, Jr. Contracting (Sullivan) of Baton Rouge, Louisiana, for $198,190. Construction of the three test lanes began on July 23, 1999 and was completed on October 1, 1999.

Normal construction practices were followed so the project would be as representative as possible of actual highway construction practices, all in accordance with *Louisiana Standard Specifications for Roads and Bridges, 1992*.

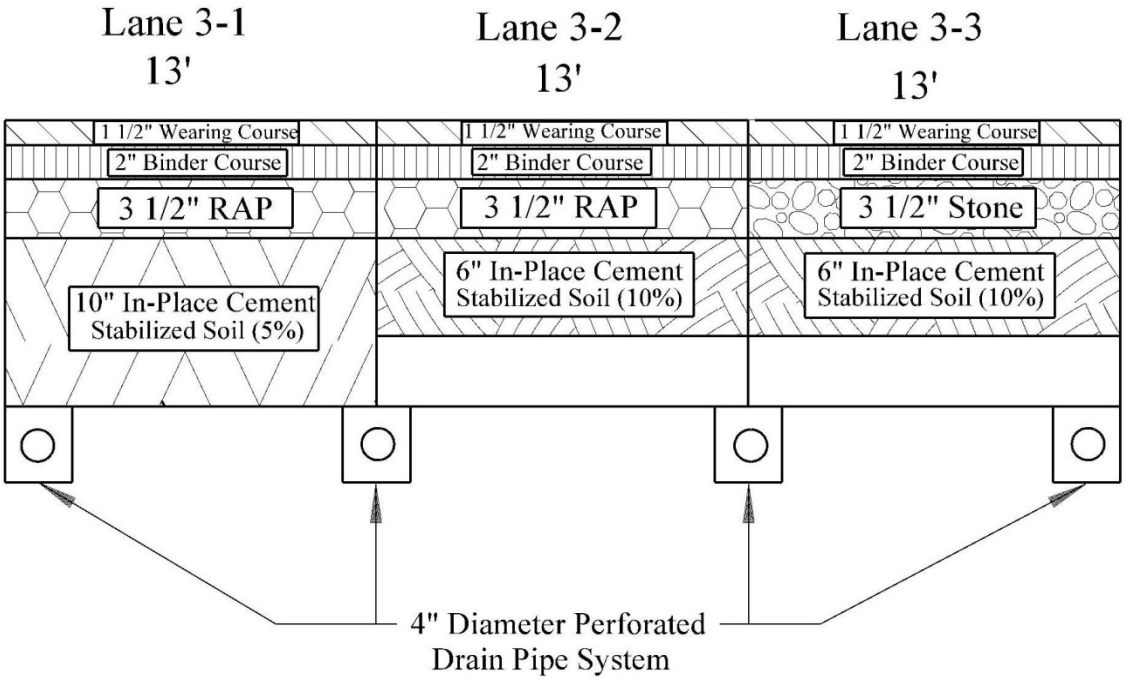

Figure 1
Test lanes cross-sections

Asphalt Materials and Mix Design

Asphalt Binders

The PAC-40 asphalt cement used for this project was supplied by Eagle Asphalt which met the Louisiana DOTD specifications. A Permatac liquid anti-strip agent was added to all of the asphalt cement at a rate of 0.8 percent by weight, as determined by Louisiana TR 322-92, which is a modified ASTM T-283 procedure.

Mix Design

Typical Louisiana Marshall mix designs were required by the contract. LADOTD specifications allow the substitution of wearing course mixes for binder course. Table 1 shows the standard Marshall properties of the mixture. The job mix design used for both the binder and wearing course in this project is detailed in Table 2. The ¾" nominal aggregate size mix design for both the binder and wearing course, using the normally specified Louisiana asphalt cement, was substituted by the contractor in August of 1999.

Table 1
Marshall Properties of Type 8 Mixture

Properties	Sample1	Sample 2	Sample 3	Sample4	Average	Spec. (6)
Spec. Gravity	2.423	2.427	2.430	2.431	2.430	
Theo. Gravity	2.593	2.592	2.592	2.592	2.592	
%Theo. Gravity	95.8	96.0	96.1	96.1	96.0	
%Voids	4.2	4.0	3.9	3.9	4.0	3-5
% VMA	13.5	13.4	13.2	13.3	13.4	13 min
% VFA	69	70	70	70	70	
Stability lbs	2570	2637	2575	2570	2588	2000 min
Flow, 1/100in	9	10	10	10	10	6-15

Table 2
Job Mix Design

HMAC Mix Designs				
Aggregate		Type 8 Binder, %	Type 8 Wearing, %	Specific Gravity
Source	Type			
Vulcan Reed	No 67 LS	43.2	43.2	2.700
Vulcan Reed	No 78	17.3	17.3	2.697
Vulcan Reed	No 11	21.1	21.1	2.701
Quick Sand	c sand	14.4	14.4	2.654
Asphalt Liquid				
Binder	Type			
AntiStrip	Perm 99	0.8	0.8	
Eagle	PAC40	4.0	4.0	1.03
TOTAL % AC		4.0	4.0	
Aggregate gradation			Gradation Required	
Sieve, mm	Sieve, in	% Passing	Type 8 Binder	Type 8 Wearing
25.00	1	100	100	100
19.00	¾	97	91-100	91-100
12.50	½	82	78-89	78-89
9.50	3/8	68	62-74	62-74
4.75	No. 4	44	33-45	33-45
2.00	No. 10	30	20-31	20-31
0.43	No. 40	14	7-15	7-15
0.18	No. 80	7	1-9	1-9
0.075	No. 200	5	2.0-5.5	2.0-5.5

The No. 67 and No. 78 coarse aggregates and the No. 11 fine aggregate were siliceous limestone supplied by Vulcan Materials Company of Gilbertsville, Kentucky. The coarse siliceous sand was supplied by Quick Sand and Gravel of Watson, Louisiana.

Base Course Materials

Two base materials were used in the ALF test lanes. The stone base used in Lane 1 consisted of 100 percent crushed limestone, which complies with the gradation specified by the LADOTD specification. The optimum moisture content for the crushed stone base is 5.9 percent, with a maximum dry density of 138.7 lbs/ft^3. The RAP base material used in Lane 2 was milled from the existing Type 8 asphalt wearing course mixtures constructed for a previous ALF project. After milling was completed, the RAP base material was stockpiled adjacent to the work area to be used in the Lane 2 construction. This RAP material was checked and complied with the gradation specified by LADOTD. The optimum moisture content is 8.6 percent, with a maximum dry density of 117.1 lbs/ft^3 (18.4 kN/m^3). Table 3 presents the gradations for both stone and RAP bases.

Table 3
Gradations for Stone and RAP Bases

Sieve, mm	RAP Base		Stone Base	
	% Passing	Specification	% Passing	Specification
63.4	100	100	100	
50.8	96.6		100	
38	96.0		100	100
25.4	92.7		94.3	
19	89.1		83.8	50-100
12.5	80.8		72.2	
9.5	71.4		65.6	
4.75	51.8	35-75	52.7	35-65
2.36	36.5		33.7	
1.18	34.0		30.6	
0.6	19.3		20.3	
0.43	13.9		18.5	10-32
0.3	9.8		17.1	
0.15	3.1		15.3	
0.075	0.45		12.9	3-15
W_{opt} (%)	8.6		5.9	
γ_{max}, pcf (kN/m^3)	117.1 (18.4)		138.7 (21.8)	

Soil Cement Subbase and Embankment Soil

An A-4 soil material was used in both the soil cement subbase and the embankment subgrade. This soil, stabilized with Type 1 cement of 10 percent by weight, was used as the subbase material for both test lanes. Table 4 presents the basic soil properties

Table 4
Soil Properties

Passing #200 (%)	Silt (%)	Clay (%)	LL (%)	PI (%)	γ_{dmax} (pcf) (kN/m^3)	w_{opt} (%)	Soil Classification		
							USCS	AASHTO	Soil type
93	70	23	28	6	108.2 (17)	16.5	CL-ML	A-4	Clay silt

Legend: AASHTO- American Association of State Highway and Transportation Officials, LL- Liquid limit, PI- Plasticity index, USCS- Unified soil classification system, w_{opt} – Optimum moisture content, opt. - Optimum, γ_d - Dry unit weight of the compacted sample.

Construction Sequence

Embankment

Construction of the new test lanes was begun by removing three existing test lanes. The three existing test lanes were removed down to the top of the existing embankment. A Case 850C dozer and Natalis 65-B motor grader were used to obtain a smooth, level embankment surface. A Hyster C727A roller was used to compact the embankment surface. Nuclear density values were obtained using a Troxler nuclear device and are reported in Table 5.

Perforated Drain Pipe System Installation

A 9" deep by 9" wide trench was constructed to facilitate the installation of the 4" perforated drain pipe system using a Case 580 backhoe/front end loader, as shown in Figure 2. An approved geotextile fabric was placed along the sides and bottom of the trench. The trench was then partially backfilled with an approved pea gravel, as shown in Figure 3. The 4" schedule 35 perforated PVC pipe was then placed, and the remainder of the trench was backfilled with the same pea gravel. The fabric was draped over the top of the trench and secured using "U" shaped spikes. Table 6 shows the gradation of the pea gravel. Prior to the construction of the subgrade, the PRF personnel began placing the pressure cell instrumentation on top of the embankment. The instrumentation plan and installation is discussed in detail in the Instrumentation section of this report.

Table 5
Nuclear Density Values of Existing Embankment

Lane No.	Station	Dry Weight Density (pcf)	Wet Weight Density (pcf)	Moisture Content, %	Percent of Compaction, %
1	0+75	112.7	129.3	14.7	103.9
	0+92.5	110.4	127.2	15.2	101.7
	1+57.5	109.5	126.5	15.6	100.9
Average Proctor					102.2
2	0+50	113.4	130.2	14.8	104.5
	0+92.5	107.9	126.0	16.9	99.4
	1+07.5	107.2	124.7	16.4	98.8
Average Proctor					100.9
3	0+75	110.7	126.6	14.3	102.1
	0+92.5	111.9	127.7	14.2	103.1
	1+57.5	107.0	124.2	16.0	98.6
Average Proctor					101.3
Average Proctor (All Lanes)					101.5

.

Figure 2
Trench excavation for perforated drain pipe installation

Figure 3
Installation of fabric and backfill

Subgrade Construction

Construction of the new test lanes continued with the placement and compaction of a 10” lift of A-4 soil material in each test lane. A Case 850C dozer was used to spread the soil at the proper depth prior to compaction. A Bomag BW172 vibratory sheep-foot roller was used to compact the A-4 soil material. Final grade was achieved using a Natalis motor grader. A Hyster C530A pneumatic roller was used to create a smooth surface on the A-4 soil prior to placing the cement.

A Type I Portland cement was placed on each of the test lanes at a rate of five percent by volume on Lane 3 and ten percent by volume on Lanes 2 and 3. A Caterpillar SS 250 stabilizer was used to process the soil cement at the proper depths. Lane 1 was mixed at a depth of 10", and Lanes 2 and 3 were mixed at a depth of 6". Initial compaction was accomplished by the Bomag sheep-foot roller followed by a Hyster steel roller.

Final grade was accomplished using a motor grader followed by the steel roller, and an MC-30 cutback asphalt prime coat was sprayed to seal the treated embankment at a rate of 0.10 gallons per square yard. Table 7 shows the nuclear density and moisture content results for the stabilized subgrade using a Troxler nuclear density gauge.

Table 6
Pea Gravel Gradation for Drainage System

Contractor		F.G. Sullivan		
Plant		AP 2		
Date		7/28/99		
Material		Pea Gravel		
Sieve	Weight,	%	% Coarse	%
1½"	0	0.00	0.00	100.00
1"	0	0.00	0.00	100.00
¾"	0	0.00	0.00	100.00
½"	0	0.00	0.00	100.00
d"	40.2	2.10	2.10	97.90
No. 4	1487.4	77.65	79.75	20.25
No. 8	347.7	18.15	99.90	2.10
No. 10	0	0.00	97.90	2.10
No. 16	27.8	1.45	99.35	0.65
No. 30	0	0.00	99.35	0.65
No. 40	0	0.00	99.35	0.65
No. 50	0	0.00	99.35	0.65
No. 80	0	0.00	99.35	0.65
No. 200	7.9	0.41	99.77	0.23
Pan	1.9			
Dec	2.6			
Total	1915.5	+ 4 Mat.	1527.6	
Initial	1912.9	Cr. Mat.	0.0	
a/wash	1910.3	% Cr.	0.0	

Base Construction

After four days of curing of the subgrade, the crushed stone was placed on Lane 3 and spread with a Case 850C dozer to a depth of 3½". Grading was accomplished using a Caterpillar motor grader, and compaction was achieved using a vibratory steel roller. Water was used to aid in the compaction effort and to achieve proper moisture content. The compaction effort was carefully monitored so that the same effort would be used to compact the RAP material. A rolling pattern was obtained by checking the density of the stone after each pass. The maximum density was achieved after three passes of the steel roller (no vibration). The optimum density for the stone was 138.0 lbs/ft^3 at 7.1 percent moisture content, as measured by the DOTD district laboratory, according to lab report number 61-147667.

Table 7
Nuclear Density Values of Cement Treated Subbase

Lane No.	Station	Wet Weight Density, (pcf)	Dry Weight Density,(pcf)	Moisture Content, %	Percent of Compaction, %
1	0+70	110.7	100.2	10.4	97.2
	0+92	110.3	-	12.2	95.3
	1+60	123.3	109.1	13.0	105.8
Average Proctor					99.4
2	0+52	106.3	95.9	10.8	93.1
	0+70	108.7	99.3	9.5	96.3
	1+12.5	110.4	99.1	11.4	96.1
Average Proctor					95.2
3	0+70	111.7	100.6	11.1	95.8
	0+92	117.2	103.1	13.7	98.2
	1+57.5	124.3	106.3	16.9	101.3
Average Proctor					98.4
Average Proctor (All Lanes)					97.6

Also after four days of curing of the subgrade, the RAP material was placed in dump trucks with a track hoe and then placed on Lanes 1 and 2. A Case 850C dozer was used to spread the RAP material to a 3½" depth. Due to the physical properties of the RAP material, compaction curves were not developed; therefore, a compaction effort similar to the stone was used. Nuclear density readings were obtained to identify the optimum compaction effort. The optimum density and moisture content of the stone was also used for the RAP material as input data for the nuclear density device, which is not a true representation of the RAP material. Therefore, RAP had a low percent of compaction as shown in Table 8. It was determined from the readings obtained that the same rolling pattern (three passes of the steel roller, no vibration) used for stone should be used for the RAP material.

Once the base was accepted, the contractor sprayed an asphaltic cement prime coat. MC-250 cutback asphalt was used to prime both the stone base and RAP base with a measured 0.25 gallons per square yard. The total material used was approximately 250 gallons, covering 1,000 square yards.

Hot Mix Asphalt Concrete (HMAC) Plant Production

Plant Mix Summary

Asphalt binder and aggregate were mixed at the contractors facility located in Port Allen, LA. The measured plant volumetric values were within Louisiana DOTD specifications.

HMAC Lay Down

Tack Coat Application. An SS-1 type of emulsion manufactured by Asphalt Products Unlimited was supplied. The dilution rate for this emulsion was 50 percent.

Table 8
Nuclear Density Values of Stone/RAP Base

Lane No.	Material	Station	Wet Weight Density (pcf)	Dry Weight Density (pcf)	Moisture Content, %	Percent of Compaction, %
1	RAP	0+54	124.9	114.3	9.3	82.8
		1+07.5	116.7	107.8	8.3	78.1
		1+62	121.9	115.0	6.0	83.4
Average Proctor						81.4
2	RAP	0+54	114.8	104.4	10.0	75.5
		1+07.5	119.4	111.5	7.1	80.8
		1+62	117.8	107.6	9.5	77.9
Average Proctor						78.1
3	STONE	0+54	140.1	133.0	5.3	96.4
		1+07.5	144.1	137.7	4.6	99.8
		1+62	138.8	131.9	5.2	95.6
Average Proctor						97.3
Average Proctor (RAP Lanes)						79.8

Equipment. A double barrel counter flow Astec plant utilized four of the five cold feed bins along with the recycling feed into the outer shell of the drum. The mixture was stored in the silo while volumetric tests and gradations were evaluated. The laboratory at the plant site was fully equipped with a Marshall hammer and stabilometer, Troxler asphalt content oven, and all necessary scales and ovens to perform required tests, including gradation analysis, AC content, and specific gravity of the mixture. This plant, located on

the north side of Highway 190 at the foot of the "Old" Mississippi River Bridge in Baton Rouge, is less than 10 miles from the ALF site. At the site, a Barber Green track paver was used to place the HMAC. The paver accepted trucks directly into its receiving hopper, since insufficient distance was available to incorporate a Material Transfer Vehicle (MTV), as required on all paving projects in Louisiana.

Compaction, Setting the Rolling Pattern. In accordance with the specifications, the contractor was responsible for determining the rolling pattern for both the binder course and wearing course. After placement of the HMAC, an Ingersoll-Rand DD90 vibratory steel roller, followed by a Bomag BW-12 rubber wheeled roller, was used for compaction. The following rolling pattern was set by the contractor: four vibratory passes, one static steel pass, three rubber roller passes, and two final passes with a static steel roller.

Post Construction Testing. Two cores from each lane were obtained and sent to the LADOTD district laboratory for analysis. Table 9 reports the measured densities and thicknesses obtained from the cores as reported by the district laboratory. An additional six cores per lane were obtained and measured by PRF personnel and are reported in Table 10. Also, elevations were taken every 10 feet at the centerline of each lane and are reported in Table 10.

Table 9
Density and Thickness of HMAC Cores

Lane No.	Layer	Sample #	Specific Gravity	Density, (pcf)	Density, % of Theo.	Thickness, * in.
1	Binder	3	2.368	147.8	97.5	2.74
		4B	2.361	147.3	97.2	2.25
	Wearing	3A	2.338	145.9	96.3	2.03
		4A	2.315	144.5	95.3	2.00
2	Binder	2	2.327	145.2	95.8	1.99
		7B	2.367	147.7	97.5	1.92
	Wearing	2A	2.292	143.0	94.4	1.54
		7A	2.293	143.1	94.4	1.51
3	Binder	1	2.371	148.0	97.7	1.73
		8B	2.374	148.1	97.8	1.95
	Wearing	1A	2.360	147.3	97.2	1.92
		8A	2.341	146.1	96.4	1.66

* Average binder thickness = 2.1 in., and the average wearing thickness = 1.78 in.

Table 10
Average Thickness by Elevation versus HMAC Cores

Type	Lane 1					Lane 2					Lane 3 (Control)				
	Elevations, in.		Core Thickness, in.			Elevations, in.		Core Thickness, in.			Elevations, in.		Core Thickness, in.		
	*Ave	*Std	Ave	Std	# of Cores	*Ave	*Std	Ave	Std	# of Cores	*Ave	*Std	Ave	Std	# of Cores
Wearing Course	1.29	.27	1.90	.16	8	1.67	.43	1.36	.14	8	1.48	.49	1.75	.20	8
Binder Course	2.02	.24	1.93	.22	8	1.62	.32	2.15	.39	8	1.95	.27	2.11	.32	8
Total	3.31	.46	3.84	.28		3.29	.57	3.51	.43		3.43	.65	3.86	.47	

* Each average elevation was based on six measurements evenly spaced along the test section.

Accelerated Pavement Testing

All of the lanes were subjected to accelerated loading by the ALF machine, which is a 94.8' long structural steel frame with a moving wheel assembly. The loading wheel travels on rails at speeds of about 10 MPH, exerting simulated traffic load on a 28' long test strip. An electric geared motor attached to the wheel generates the wheel load movement. At the ends of the frame, the rails curve upward to permit gravity to accelerate, decelerate, and change the direction of the wheel assembly. Loads are applied to the pavement in one direction by the dual truck tire assembly, representing the real traffic load, and can be distributed laterally to simulate traffic wander, producing the wheel path observed on the highway.

The ALF machine, as seen in Figure 4, can apply approximately 380 load cycles per hour. The loads applied to the pavement can be varied by the operators from dead weight of 9,750 lbs (43.4 kN0) to 21,250 lbs (111.25kN) by adding load plates. The loading schedule of all the lanes is shown in Table 11.

Figure 4
ALF machine

The loading was applied alternatively between the test lanes in 25,000 pass increments in an attempt to minimize the relative environmental effects occurring during the loading period. Rutting of 0.50- .75". (12.7- 19.05 mm) was defined as the failure condition for the pavement. Once the rutting failures occurred, the testing was stopped, and the number of loads to failure was determined. Secondary testing on the pre-cracked subgrade was initiated after completion of testing on the original sections.

Field Measurements

Field measurements included the periodic collection of cracking, transverse and longitudinal profile, deflection data, and temperatures. The ALF loading was stopped periodically for maintenance, and surface measurements were made at those times. Each of the lanes had the transverse profile measured after each increment of 25,000 load applications.

For the transverse profile, eight profile measurement stations were located at 4' (1.22-m) intervals along the 35' (10.67-m) test lane. The profile data were secured using the ALF profilograph, which consists of a linear variable differential transformer (LVDT) mounted on a metal carriage. It moves transversely across the pavement on a metal frame. The metal frame can be positioned along the pavement section between two rails mounted on the pavement surface, outside the trafficked area. A rut depth is calculated from each transverse profile. Maximum rut depth was also determined using the manual AASHTO rut measuring device.

Deflection testing was conducted on a periodic basis using the falling weight deflectometer (FWD) and the Dynaflect. The FWD (Figure 5) data were used to backcalculate the moduli of each layer of the test sections. Applying an impulse force generated from two mass assemblies in which the falling weight was dropped onto a second weight/buffer combination created the deflection measurement. The measurements with each device were performed on the centerline of the loading path of each pavement test section at eight stations spaced at intervals of 4' (1.22-m) along the centerline.

The deflections through Dynaflect (Figure 6) are achieved by five sensors impacted by the Dynaflect loading system. Dynaflect is a trailer-mounted device that induces a 1,000 lb. dynamic load on the pavement. It then measures the resulting slab deflections through the use of five geophones spaced under the trailer at approximately one foot intervals from the application of the load. The 1,000 lb. dynamic load is generated at a frequency of eight cycles per second by the counter-rotation of two unbalanced fly-wheels. This cyclic force is transmitted vertically to the pavement through two steel wheels spaced 20 inches center to center. The horizontal reaction forces cancel themselves due to the opposing rotations. The dynamic force varies in sine wave fashion from 500 lbs., upward to 1000 lbs., downward

during each rotation and resulted in a total force of 1,100 to 2,100 lbs. Applied to the pavement with the inclusion of the trailer assembly weight. Figure 6 shows this device during a test. Dynaflect is designed to simulate dynamic loads exerted on the pavement by the moving truck traffic. The deflections are measured in milli-inches (thousandths of an inch), similar to fwd.

Table 11
Load History for Experiment III

No. of Passes x 1000	Applied Load, Lbs.	Cumulative Load, ESALs	Start Lane 1 Date	End Lane 3 Date	
0 – 25	9,750	34,434	3/17/01	4/16/01	
25 – 50	9,750	68,868	4/20/01	7/24/01	
50 – 75	9,750	103,302	7/25/01	8/17/01	
75 – 100	9,750	137,736	8/21/01	9/26/01	
100 – 125	9,750	172,170	9/28/01	10/20/01	
125 – 150	9,750	206,604	10/22/01	11/21/01	
150 – 175	9,750	241,038	11/27/01	02/12/2	
175 – 200	9,750	275,473	02/14/02	05/20/02	
200 – 225	12,050	355,810	05/23/02	10/17/02	
225 – 250	12,050	436,147	10/25/02	11/18/03	
250 – 275	12,050	516,484	01/21/03	02/11/03	
275 – 300	12,050	596,821	02/13/03	03/18/03	
300 – 325	12,050	677,158	03/23/03	04/23/03	
325 – 350	12,050	757,495	04/23/03	05/28/03	
350 – 375	12,050	837,832	06/02/03	06/26/03	
375 – 400	12,050	918,169	06/30/03	07/26/03	
400-425	12,050	998,494	08/06/03	08/21/03	
425-450	12,050	1,078,819	08/21/03	09/07/03	
450-475	12,050	1,159,144	09/10/0/3	10/13/03	L2 Failed @ 450,300
475-500	12,050	1,239,469	10/23/03	11/03/03	L1 & L3 Only
500-525	12,050	1,319,794	11/04/03	11/11/03	L1 & L3 Only
450-525	12,050	1,319,794	12/22/03	01/13/04	L2 Only
525-550	14,350	1,481,369	01/13/04	01/30/04	All Lanes
550-575	14,350	1,642,944	02/04/04	02/29/04	
575-600	14,350	1,804,523	03/01/04	04/23/04	
600-625	14,350	1,966,099	04/23/04	05/20/04	
625-650	14,350	2,127,675	05/20/04	06/16/04	
650-675	14,350	2,289,252	06/17/04	07/07/04	

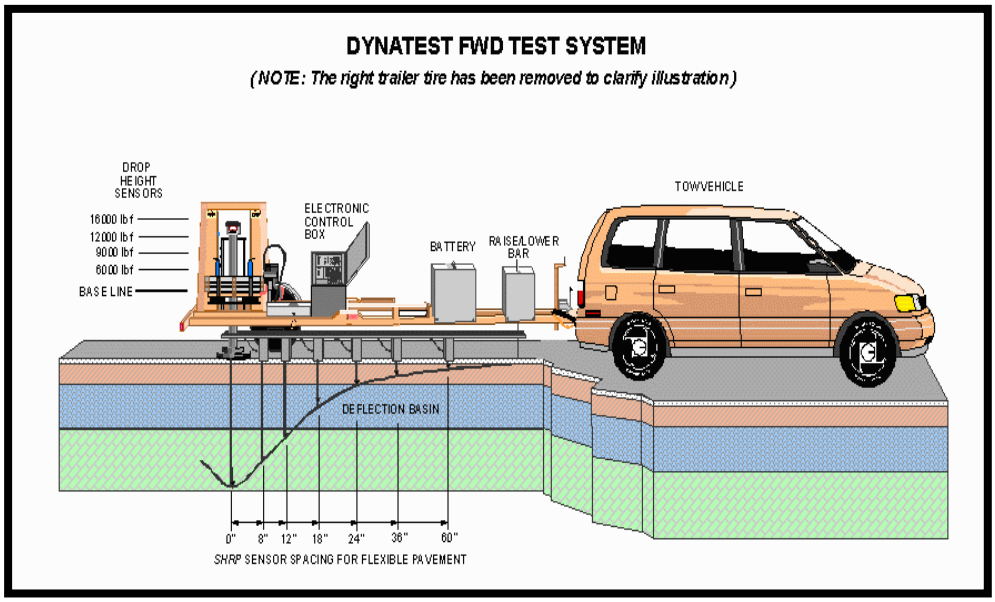

Figure 5
FWD illustration

Figure 6
Dynaflect device

Density of the asphalt cement layer of test lanes was measured with a nondestructive device, Pavement Quality Indicator (PQI). The device has a circular base plate housing a transmitter at the center that emits an electrical flow into the asphalt material. An isolation ring surrounds the transmitter, and a receiver circumscribes the isolation ring along the outer perimeter of the base plate. The electrical flow passes through the asphalt pavement in a toroidal electrical sensing field. The density is measured by the response of the PQI's electrical sensing field to changes in electrical impendence of the material matrix, which in turn is a function of the composite dielectric constant of the paving material and the air trapped in the voids of the material. In this study, density measurements were performed approximately every 25,000 applications of the ALF axle load, and five measurements were taken at each pavement test point.

Weather Data Collection

A Campbell Scientific weather station installed at the site was used to collect weather related data such as air temperature, relative humidity, wind direction and speed, solar energy, barometric pressure, and rain fall during the test period.

Laboratory Evaluation

Asphalt Mixture

In the laboratory, asphalt mixture was characterized using fundamental engineering property tests. These tests included the indirect tensile strength (ITS), indirect tensile resilient modulus (MR), indirect tensile creep (IT-CRP), axial creep (AX-CRP), Superpave frequency sweep at constant height (FSCH), and repetitive shear at constant height (RSCH) tests. Asphalt mixture specimens for the tests listed above were prepared using the U.S. Army Corps of Engineers Gyratory Testing Machine (GTM) and the Superpave Gyratory Compactor (SGC) from plant produced materials. There were two specimen sizes: 4.0 " (101 mm) in diameter by approximately 2.5" (63 mm) in height made from GTM and 6.0" (150 mm) in diameter by approximately 4.7" (120-mm) in height made from the SGC. The 6.0" (150 mm) diameter specimens made by the SGC were cut into 2.0" (50 mm) thick specimens for the Superpave shear tester (SST) protocols. At the target air void levels (7 percent for the SST tests and 4 percent for the other tests), specimens were statistically grouped in triplicate sets to have similar mean air void levels. Indirect tensile strength (ITS) tests at 77^{o}F (25^{o}C); indirect tensile resilient modulus (MR) tests at temperatures of 40, 77 and 104^{o}F (4, 25, 40^{o}C); and indirect tensile creep (IT-CRP) and axial creep (AX-CRP) tests at 104^{o}F (40^{o}C) were conducted. In addition, the Superpave frequency sweep at constant height (FSCH) test was conducted to determine viscoelastic properties of the asphalt mixtures that include dynamic shear modulus (G*) and shear phase angle (δ) at 140^{o}F (60^{o}C). Repeated shear test at

constant height (RSCH) was used to evaluate permanent deformation behavior of the asphalt mixture. Table 12 presents the tests performed for designed mixture. Since wearing course and binder course use the same type 8 mixture, only one mixture was tested.

Table 12
Test Factorial for Mixture Characterization

Tests	Sample Size Diameter × Height		Test Temperature		Type 8 Binder Course, Wearing course
	inch	mm	°F	°C	
ITS[1]	4.0 ×2.5	101×63	77	25	3
M_R[2]	4.0 ×2.5	101×63	40,77,104	5,25,40	3 ,3 ,3
IT-CRP[3]	4.0 ×2.5	101×63	104	40	3
AX-CRP[4]	4.0 ×2.5	101×63	104	40	3
FSCH[5]	6.0 ×2.0	150×50	140	60	3
RSCH[6]	6.0 ×2.0	150×50	140	60	3

1 Indirect tensile strength test
2 Indirect tensile resilient modulus test
3 Indirect tensile creep test
4 Axial creep test
5 the Superpave frequency sweep at constant height test
6 repeated shear test at constant height

Indirect Tensile Strength (ITS) Test. The indirect tensile strength (ITS) and strain test was used to determine the tensile strength and the evolution of the strain of the mixtures. This test was conducted at 77°F (25°C), according to AASHTO T245 (7). Each test specimen was loaded to failure at a 2" per min. (50.8 mm/min) deformation rate. The load and deformations were continuously recorded, and indirect tensile strength and strain were computed as follows:

$$S_T = \frac{2 \cdot P_{ult}}{\pi \cdot t \cdot D} \quad (1)$$

$$\varepsilon_T = 0.205 H_T \quad (2)$$

where,

S_T = tensile strength, kPa;

P_{ult} = peak load, N;

t = thickness of the specimen, mm;

D = diameter of the specimen, mm;

ε_T = horizontal tensile strain at failure, mm/mm; and

H_T = horizontal deformation at peak load, mm.

The Toughness Index (TI) is a parameter that describes the toughening characteristics in the post-peak region. It is computed from the indirect tensile test results. Figure 7 presents a typical normalized indirect tensile stress and strain curve. A dimensionless indirect tensile toughness index, TI, is defined as follows:

$$TI = \frac{A_{\varepsilon} - A_{p}}{\varepsilon - \varepsilon_{p}} \tag{3}$$

where,

TI = toughness index;

Aε = area under the normalized stress-stain curve up to strain ε;

A_p = area under the normalized stress-stain curve up to strain ε_p;

ε = strain at the point of interest; and

ε = strain corresponding to the peak stress.

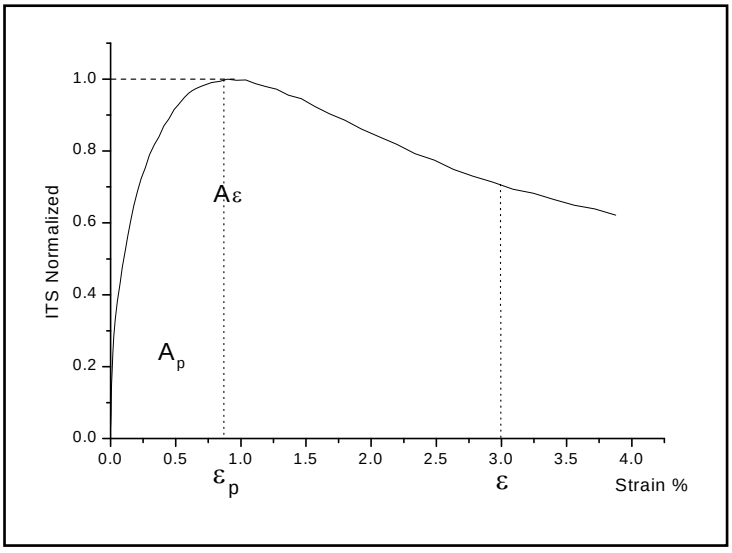

Figure 7
A typical normalized ITS curve for toughness index calculation

The toughness index compares the performance of a specimen with that of a perfectly plastic reference material for which the TI remains a constant of 1. For an ideal brittle material with no post-peak load carrying capacity, the value of TI equals zero.

Indirect Tensile Resilient Modulus (MR) Test. This test was conducted according to the modified ASTM D 4123 at test temperatures of 40, 77, and 104°F (4, 25, and 40°C) *(3).* This test is a repeated load indirect tension test for determining the resilient modulus of the asphalt mixtures. The recoverable vertical deformation δV and horizontal deformation δH

were used to calculate the indirect tensile resilient modulus, M_R and Poisson's ratio, as shown in Equations 4 and 5.

$$M_R = \frac{P \cdot (\mu + 0.27)}{t \cdot \delta H} \tag{4}$$

$$\mu = 3.59 \cdot \frac{\delta H}{\delta V} - 0.27 \tag{5}$$

where,
M_R = Resilient Modulus, MPa;
P = applied vertical load, N;
T = sample thickness, mm;
M = Poisson's ratio;
δH = horizontal deformation, mm; and
δV = recoverable vertical deformation, mm.

Indirect Tensile Creep (IT-CRP) Test. At 104°F (40°C), a compressive load of 250 lbf (1.110 kN) was applied to the specimen using the stress-controlled mode of the MTS test system. The load was applied for 60 minutes or until the specimen failed *(2)*. The deformations acquired during this time were used to compute the creep modulus as follows:

$$S(T) = \frac{3.59 \cdot P}{t \cdot \delta V(T)} \tag{6}$$

where,
S(T) = creep modulus at time T, MPa;
P = applied vertical load, N;
T = sample thickness, mm; and
δV(T) = vertical deformation at time T, mm.

Figure 8 shows a typical creep modulus versus time graph on a log-log scale for the indirect tensile creep data. The graph slope was computed from this graph and used in the analysis.

Axial Creep (AX-CRP) Test. This test was conducted in accordance with the test method Tex-231-F. A static load of 125 lbf (0.555 KN) was applied for the duration of one hour along the centric longitudinal axis of the specimen. The axial deformation of the specimen is continuously measured and subsequently used to calculate creep properties such

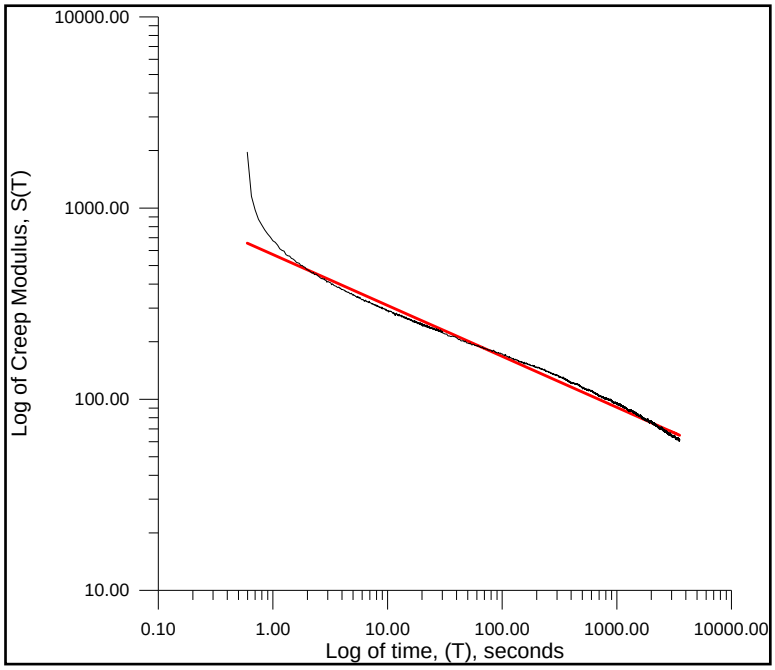

Figure 8
Typical curve of IT creep modulus

as stiffness, slope, and permanent strain. These data are used to evaluate the permanent deformation characteristics of asphalt mixtures. Figure 9 presents a typical creep curve from the axial creep test.

Frequency Sweep at Constant Height (FSCH) Test. This test, conducted in the shear mode (Figure 10), is a strain-controlled test in which a specific amount of deformation is induced in the specimen at 140°F (60°C). Stress generated in the specimen is measured but not controlled. The sinusoidal shear strain with peak amplitude of approximately 0.05 inch/inch (i.e. 50 micro strain) is applied at frequencies of 10, 5, 2, 1, 0.5, 0.2, 0.1, 0.05, 0.02, and 0.01 Hz. This strain level was selected during the SHRP research program to ensure that the viscoelastic response of the asphalt mixture is within the linear range, meaning that the ratio of stress to strain is a function of loading time (or frequency) and not of the stress magnitude. An axial stress is applied to maintain constant height. Frequency is directly related to traffic speed. For example, a frequency of 1 Hz corresponds to a traffic speed of 39 miles/hr. (63 km/hr) *(4).* Hence, a frequency sweep test can be used to evaluate the behavior of an asphalt mixture at different traffic speeds. Figure 11 presents typical load curves of an FSCH test.

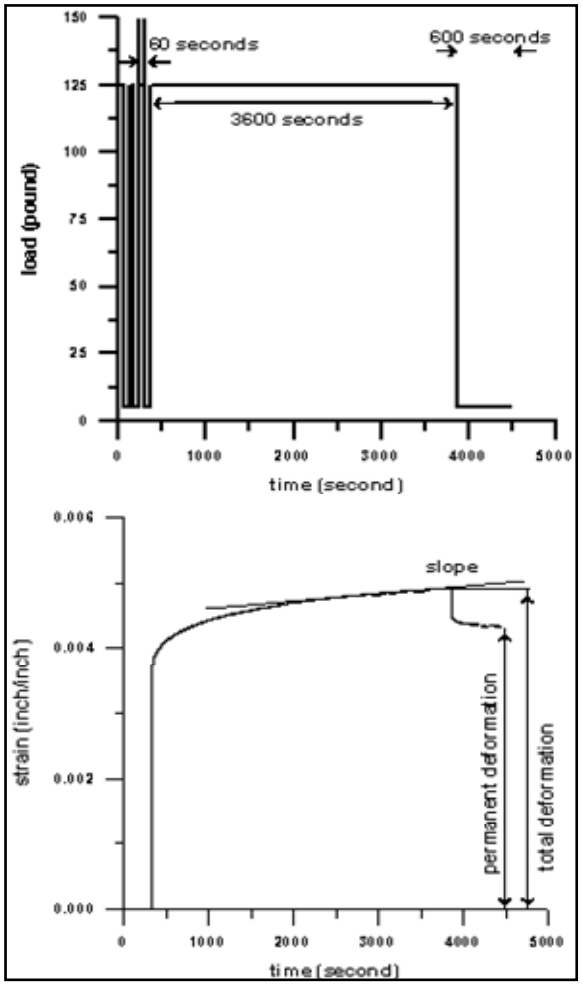

Figure 9
A typical axial creep curve

Figure 10
Frequency Sweep at Constant Height (FSCH) test equipment

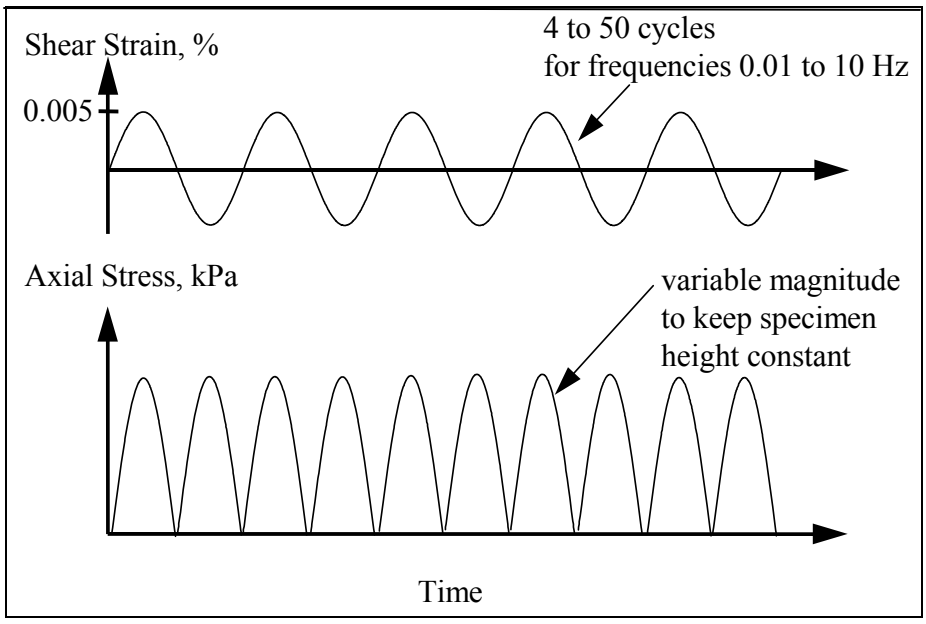

Figure 11
Shear strain and axial stress applications in FSCH test

Repetitive Shear at Constant Height (RSCH) Test. This is a stress-controlled test. A repetitive shear load (haversine) is applied to the specimen to generate a shear deformation. The shear load is applied with a maximum shear stress of 10 psi (68 kPa) for a loading time of 0.1 seconds and a rest period of 0.6 seconds. Repetitive loading is applied for a total of 5,000 repetitions or until 5 percent shear strain occurs. An axial stress is applied to maintain constant height.

In development of the repeated shear test at constant height, two mechanisms that provide resistance to permanent deformation in an asphalt mixture were hypothesized :

1. Asphalt binder stiffness — Stiffer binders help in resisting permanent deformation as the magnitude of the shear strains is reduced under each load application. The rate of accumulation of permanent deformation is strongly related to the magnitude of the shear strains. Therefore, a stiffer asphalt will improve rutting resistance as it minimizes shear strains in the aggregate skeleton.

2. Aggregate structure stability — The axial stresses act as a confining pressure and tend to stabilize the mixture. A well-compacted mixture with a good granular aggregate will develop high axial forces at very small shear strain levels. Poorly compacted mixtures can also generate similar levels of axial stresses, but they will experience much higher shear strain.

In the constant height simple shear test, these two mechanisms are free to fully develop their relative contribution to the resistance of permanent deformation, as they are not constrained by imposed axial or confining stresses. The development of the repeated shear test at constant height was detailed elsewhere (5). Figure 12 shows the typical load curves of RSCH tests.

Base Course Material

The resilient modulus of both RAP and crushed stone base course material were determined in the laboratory using the repeated load triaxial test.

Repeated Load Triaxial Test (Resilient modulus test). This test was conducted according to the American Association of State Highway and Transportation Officials (AASHTO) test procedure, T294-94 “Resilient Modulus of Unbound Granular Base/Subbase Materials and Subgrade Soils.” The resilient modulus (M_r) in a repeated load test is defined as the ratio of the maximum deviator stress (σ_d) to the recoverable elastic strain (ε_r) as follows:

$$M_r = \sigma_d/\varepsilon_r \quad (7)$$

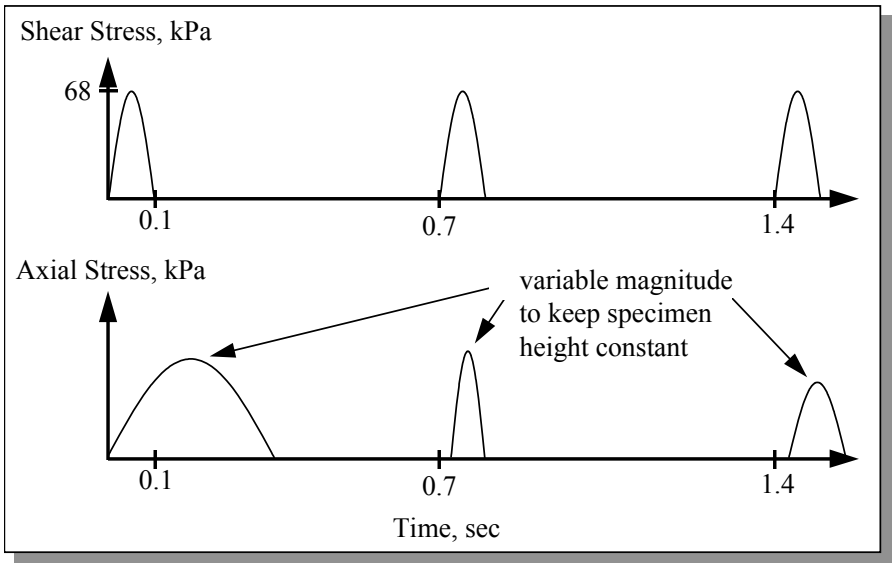

Figure 12
Shear and axial stress during Repetitive Shear at Constant Height test

The 152.4 mm (in diameter) x 304.8 mm (in height) samples were compacted in a laboratory using an electric vibrator. The samples were conditioned through the application of 1,000 repetitions of a specified deviator stress and were then subjected to different stress levels. The stress levels were selected to cover the expected in-service range that a pavement material experiences under traffic.

DISCUSSION OF RESULTS

This section consists of two parts, laboratory tests and field measurements. Laboratory tests include Indirect Tensile Strength Test, Indirect Tensile Creep Test, Indirect Tensile Resilient Modulus Test, Axial Creep Test, Frequency Sweep at Constant Height Test, Simple Shear Test at Constant Height Test, and Resilient Modulus Test. Field experimentation includes the conduct of accelerated loading tests on all three different lanes and compares their pavement performance. Field measurements include rutting, nondestructive testing (Dynaflect, FWD), and density.

Laboratory Test Results

Asphalt Mixture

In an effort to evaluate the asphaltic concrete of the ALF 3 test section, HMAC samples were collected on the plant, and mechanistic tests were conducted, including Indirect Tensile Strength Test, Indirect Tensile Creep Test, Indirect Tensile Resilient Modulus Test, Axial Creep Test, Frequency Sweep at Constant Height Test, and Simple Shear at Constant Height Test. Each test was conducted with three replicates, and standard statistical index, such as average, standard deviation, and CV%, was employed to test the variability of the experimental values.

Indirect Tensile Strength (ITS). Table 13 presents the test results of the indirect tensile strength (ITS), the corresponding strain at failure, and the toughness index (TI) at 25°C (77°F), along with their mean, standard deviation, and CV%. The ITS values of the tested mixture are higher than the type 8 wear course with PAC 40 used in the ALF 2 Experiment, while the TI is lower than that of the type 8 mixture (1).

Table 13
Indirect Tensile Strength (ITS) results

Sample ID	Air Voids	ITS		IT Strain	TI
		psi	Mpa		
1	4.1	366	2.53	0.51	0.34
2	4.2	388	2.68	0.42	0.32
3	3.9	365	2.52	0.30	0.29
AVG.	4.1	373	2.57	0.41	0.32
STD	0.2	13	0.089	0.11	0.02
CV%	3.8	3.5		26.3	7.9
Type 8 Wearing Course with PAC 40 (1)		203	1.40	0.56	0.51

Indirect Tensile Resilient Modulus (M_R). Table 14 presents the mean indirect tensile resilient modulus at 40, 77 and 104 °F (4, 25 and 40 °C), along with their standard deviation and CV%. As expected, the modulus values decrease with the increase of temperature. And the resilient modulus of tested mixture is higher than that of type 8 wear course mixture with PAC 40 used in ALF 2 Experiment (1) at all three test temperatures, which is consistent with the indirect tensile strength test results.

Table 14
Indirect Tensile Resilient Modulus (M_R)

Temperature		Average M_R		STD	CV%	Type 8 Wearing Course with PAC 40 (1)	
°C	°F	ksi	Gpa			ksi	Gpa
4	44	829	5.72	91.09	11.0	633	4.37
25	77	769	5.31	37.71	4.9	464	3.20
40	104	569	3.92	61.91	10.9	286	1.97

Indirect Tensile Creep (IT-CRP) Results. Table 15 presents the Indirect Tensile Creep Tests results at 40°C (104°F), along with their mean, standard deviation and CV%. It should be noted that compared to type 8 wear course mixture used in ALF 2 Experiment (1), the tested mixture exhibits lower creep slope and longer time to failure, which indicates a higher rutting resistance property for the tested mixture. And this observation is consistent with the results of indirect tensile strength and indirect tensile resilient modulus tests.

Table 15
Indirect Tensile Creep (IT-CRP) Results

Sample ID	Air Void (Percent)	Slope (log psi/log second)	Time at Failure (Second)
1	4.0	0.35	1871
2	4.5	0.31	3600
3	4.1	0.30	3600
AVG.	4.2	0.32	3024
STD	0.3	0.03	998
CV%	6.3	8.27	33.0
Type 8 Wearing Course with PAC 40 (1)		0.40	1040

Axial Creep (AX-CRP) Test Results. Table 16 presents the Axial Creep Tests results at 40°C (104°F). It shows that the single and average values of creep stiffness and permanent strain of all three samples meet the requirements set by Texas specification (6000 psi Min, 5.0E-04 Max) while the creep slopes for all the samples are beyond the specified value (3.5E-08 Max).

Table 16
Axial Creep (AX-CRP) Results

Sample ID	Air Void	Creep Stiffness (psi)	Slope 1/Second ($\times 10^{-8}$)	Permanent Stain ($\times 10^{-4}$)	Total Stain ($\times 10^{-3}$)
12	3.7	6747	10.8	4.4	1.5
17	4.0	8583	10.3	4.9	1.2
19	4.1	9477	11.8	3.2	1.1
AVG.	3.9	8269	11.0	4.2	1.2
STD	0.2	1392	0.8	0.9	0.2
CV%	5.3	16.8	6.8	20.8	17.6
Texas Spec (3)		>6000	<3.5	<5.0	

Frequency Sweep at Constant Height (FSCH) Results. Table 17 presents the Frequency Sweep at Constant Height (FSCH) test results at 60°C, including complex shear modulus G*, phase angle δ, and rut parameter G*/Sinδ along with their means, standard deviations and coefficient variations CV%.

Figure13 presents the complex shear modulus G* versus frequency from the frequency sweep at constant height test.

In order to analyze the temperature sensitivity of FSCH data, the regression method is used to explore the relationship between complex shear complex modulus G* and loading frequency f. And it is found that a polynomial regression equation as follows can fit the G* and f data very well in some studies (8).

$$log\ (G^*) = C_0\,(log\ f)^2 + S_0\,(log\ f) + G_0 \qquad (8)$$

where,
G* = complex shear complex modulus, kPa;
F = loading frequency, Hz; and
C_0, S_0 and G_0 = regression constants.

Table 17
Frequency Sweep at Constant Height (FSCH) Results

Complex Shear Modulus G* (ksi)										
Frequency	0.01	0.02	0.05	0.1	0.2	0.5	1	2	5	10
Sample 1	2.746	3.05	3.487	3.939	4.645	6.007	7.48	9.432	12.514	17.155
Sample 2	2.983	3.265	3.695	4.157	4.83	6.17	7.621	9.699	12.789	17.734
Sample 3	2.011	2.174	2.455	2.777	3.261	4.156	5.275	6.921	9.707	13.887
AVG.	2.58	2.83	3.212	3.624	4.245	5.444	6.792	8.684	11.67	16.259
STD	0.507	0.578	0.664	0.742	0.857	1.119	1.315	1.533	1.705	2.074
CV%	20	20	21	20	20	21	19	18	15	13
Phase Angle δ										
Frequency	0.01	0.02	0.05	0.1	0.2	0.5	1	2	5	10
Sample 1	22.5	24.1	26.8	29.4	31.4	35.3	37.1	39.1	43.1	43.4
Sample 2	24.9	25.8	28.2	30.1	32.5	36.9	38.6	40.9	45	44.6
Sample 3	25.4	26.6	29.3	31.3	34.4	38.3	41.2	42.6	46.4	46.3
AVG.	24.3	25.5	28.1	30.2	32.8	36.8	38.9	40.8	44.9	44.7
STD	1.5	1.3	1.3	1.0	1.5	1.5	2.1	1.85	1.7	1.5
CV%	6	5	4	3	5	4	5	4	4	3
G*/Sin δ (×1000)										
Frequency	0.01	0.02	0.05	0.1	0.2	0.5	1	2	5	10
Sample 1	7.196	7.46	7.727	8.032	8.903	10.385	12.414	14.96	18.303	24.98
Sample 2	7.095	7.491	7.811	8.3	8.986	10.284	12.217	14.826	18.079	25.276
Sample 3	4.692	4.851	5.01	5.351	5.767	6.712	8.012	10.224	13.396	19.203
AVG.	6.319	6.601	6.849	7.228	7.885	9.127	10.881	13.337	16.592	23.153
STD	1.409	1.515	1.593	1.631	1.835	2.092	2.478	2.696	2.771	3.424
CV%	22	23	23	23	23	23	23	20	17	15

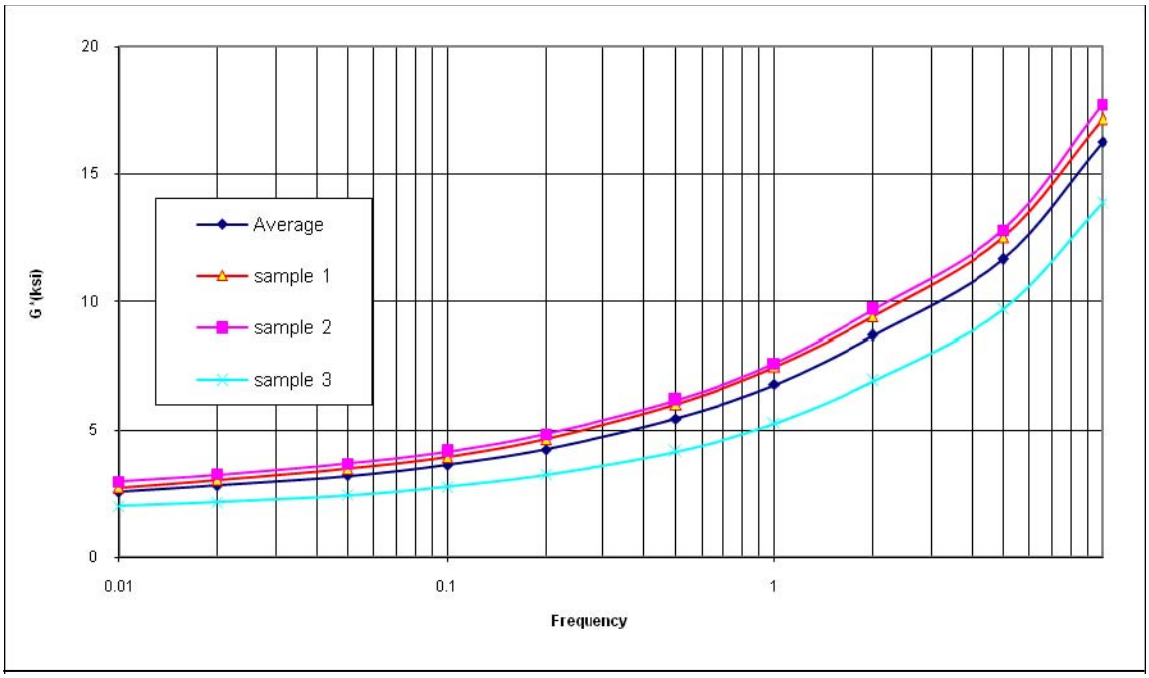

Figure 13
Complex shear modulus of FSCH test

As shown in Figure 14, the polynomial equation fits the average value of FSCH test data very well. In fact, all FSCH test data obtained in this study were found to have a R^2 value greater than 0.99 by the use of this polynomial regression method. Therefore, in order to discriminate different test data, another material parameter, the critical complex shear modulus (G^*_{crit}) is introduced to analyze the FSCH test data (8). Based on the minimum G* value found in Equation (8), G^*_{crit} can be calculated by the following equation:

$$G^*_{crit} = 10^{G_0 - \frac{S_0^2}{4C_0}} \quad (9)$$

where, C_0, S_0 and G_0 are the same parameters used in Equation (8).

Since the computation of the G^*_{crit} value takes all three material constants in Equation (8) into account, it is thought that this parameter is a better representative for the FSCH test results than any single stiffness value obtained under any test frequencies.

Table 18 presents the calculated critical complex shear modulus, G^*_{crit}, of the tested mixture. Compared to the other two mixtures, Mix CS1-1 and Mix CS1-2 (Mix CS1-1 is a dense-graded mixture with a crumb rubber (Rouse 80 mesh powdered rubber) modified (CRM) binder; Mix CS1-2 is a gap-graded mixture with a SB polymer (SB Poly) modified binder) used in reference , the G^*_{crit} value of the tested mixture is higher as shown in Table 18, which implies a better rut resistance property.

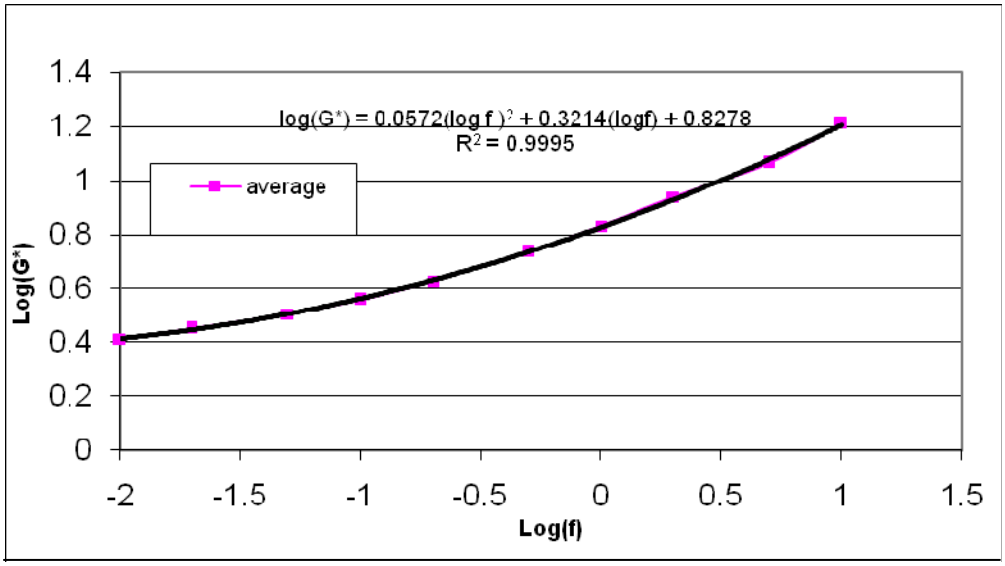

Figure 14
Typical variation of shear complex modulus vs. frequency

Table 18
The Critical Complex Shear Modulus

Mixture		C0	S0	G0	R^2	G*crit,	
						kPa	ksi
This experiment	Type 8	0.0572	0.3214	0.8278	0.9995	16412	2.378
Reference (8)	CS1-1	0.0586	0.3438	4.573	0.9996	11712	1.697
	CS1-2	0.0678	0.2957	4.429	0.9998	12788	1.853

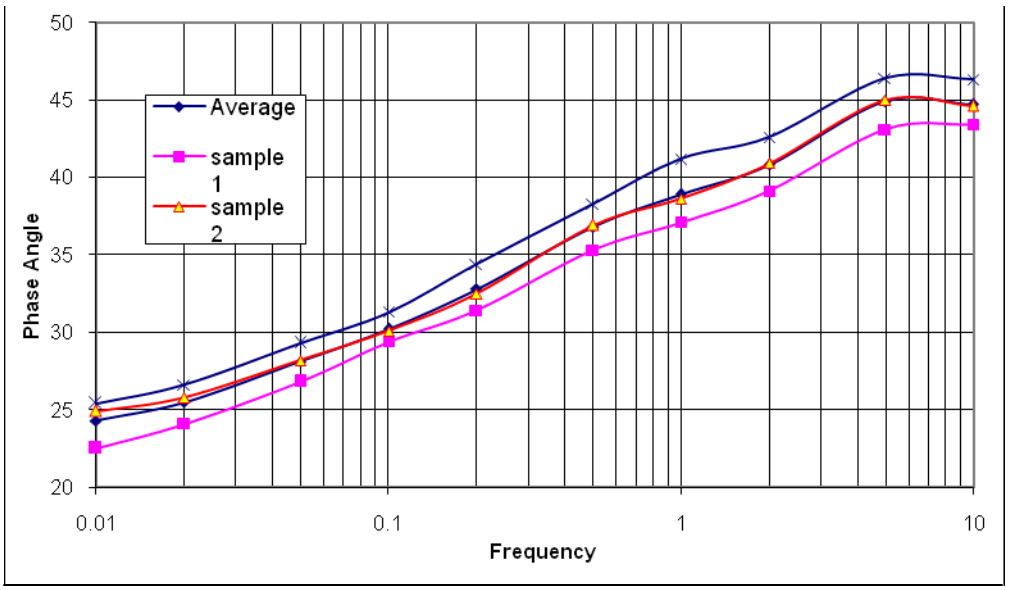

Figure 15
Phase angle of FSCH test

Figure 15 presents phase angle versus frequency from the frequency sweep at constant height test. Generally, the phase angle δ of asphalt binder will decrease as the frequency increases in the FSCH test, but it shows that the phase angle δ of tested mixture increases as the frequency increases, which means that at test temperature (60 °C), the contribution of asphalt binder to phase angle is insignificant, and aggregate plays a dominant role in determining the phase angle of mixture, and this results in the increase of phase angle with the increase of frequency. But it should be noted that the increasing trend is not indefinite; there is a peak value for phase angle around frequency 5, and as the frequency continues increasing, the phase angle of tested mixture will decrease accordingly.

Figure 16 presents the complex modulus G* versus phase angle for the average value of the three samples. It shows that the phase angle of tested mixture increases with the increase of complex modulus, and after reaching a peak value it decrease. This can be explained by the same reason previously discussed.

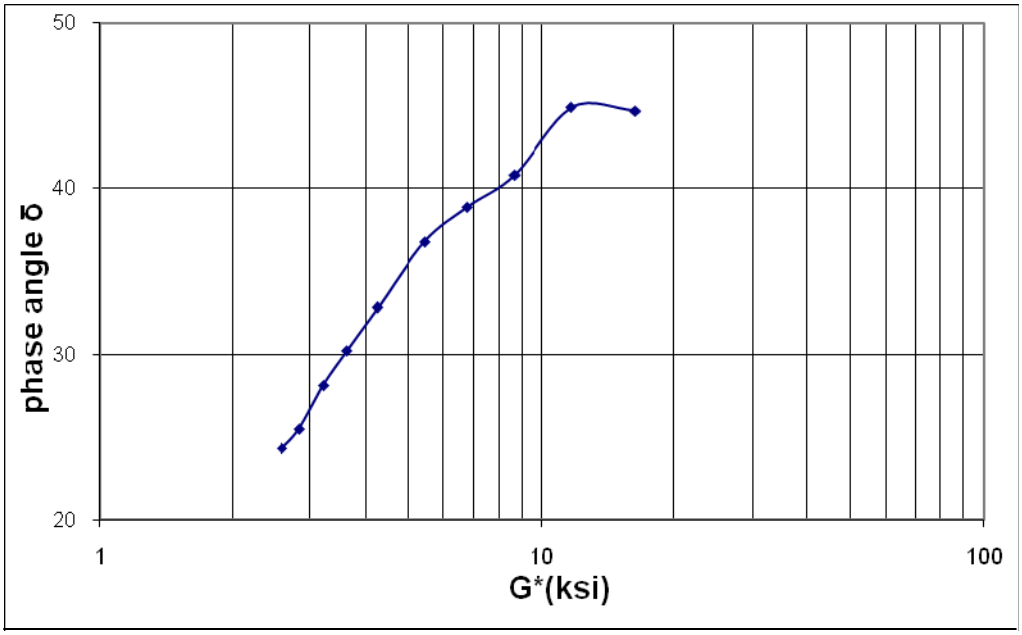

Figure 16
G* versus phase angle δ of FSCH test

Repeated Shear at Constant Height (RSCH) Test. Figure 17 presents the permanent strain versus loading cycles of Superpave simple shear at constant height test at 60°C (140°F), along with the permanent shear stain values of all three sample as well as their mean, standard deviation and CV% at 5,000 cycles. It shows that the permanent strains at 5,000 cycles of all three samples are below the specified value 0.05.

Figure 18 compares the permanent stain of Type 8 wearing/ binder course mixture for ALF 3 to conventional Type 8 mixture and Type 8 with PRM wearing course mixture for ALF 2 *(1)*. It shows that the permanent strains at 5,000 cycles of all the three mixtures are far below the specified value 0.05, which reflects that all the three mixtures possess an excellent permanent deformation– resistant property.

One application of RSCH results is to estimate the rut depth of the asphalt concrete layer composed of the tested mixture with the plastic shear strain *(9)*. The rut depth can be calculated using the following empirical equation:

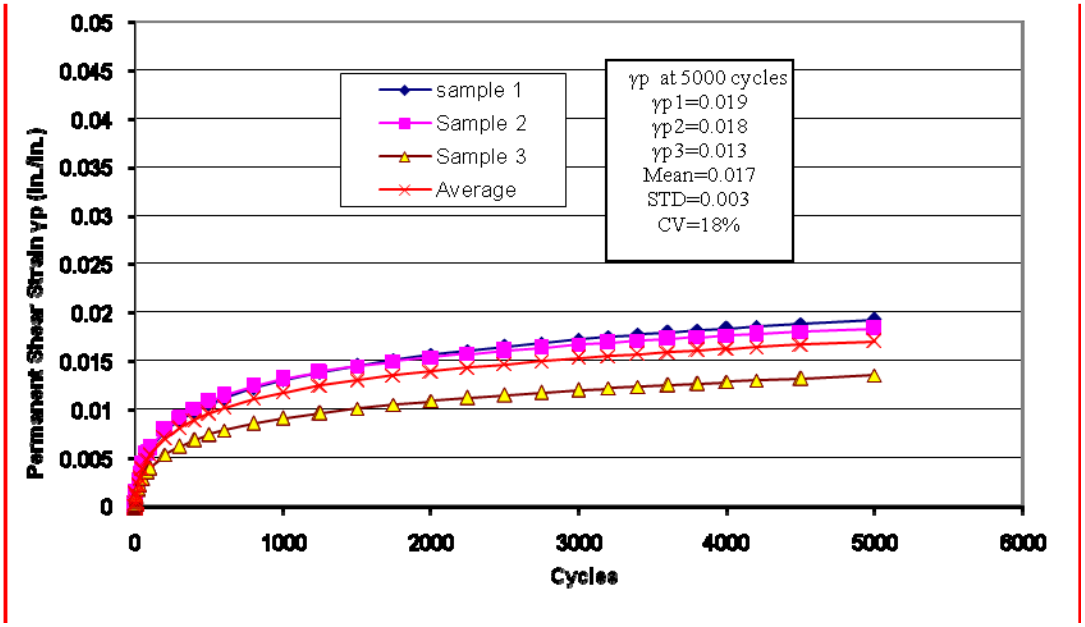

Figure 17
Permanent strain of RSCH test

Rut depth = A * max. permanent shear strain

- A= 11, rut depth in inch

With this equation, the estimated rut depth of AC layer in this project is

Rut depth = 0.017*11=0.187"

This value is an estimator of the rut depth of the AC layer at equivalent experimental condition (60 °C, 5,000 cycles). Compared to the rut depth measured at the end of loading history (after 1,803 ESAL) on the ALF site, this value is similar with the result of lane 1 (0.16inch), and smaller than those of lanes 2 and 3 (0.36" and 0.46", respectively).

Base Course Material

Resilient Modulus Test. Table 19 presents the mean resilient modulus of crushed stone and RAP material, along with their standard deviation, CV% and t-tests results. It shows that the mean resilient modulus of RAP material is higher than that of crushed stone, but RAP also has a higher CV. Therefore, a student t-test method was used to compare those M_r values. The high p-value (0.1515 > 0.05) of the t-test indicates that there is no significant difference between the resilient modulus of RAP and crushed stone materials. This statistical similarity in lab results implies a comparative performance of RAP and crushed stone in field.

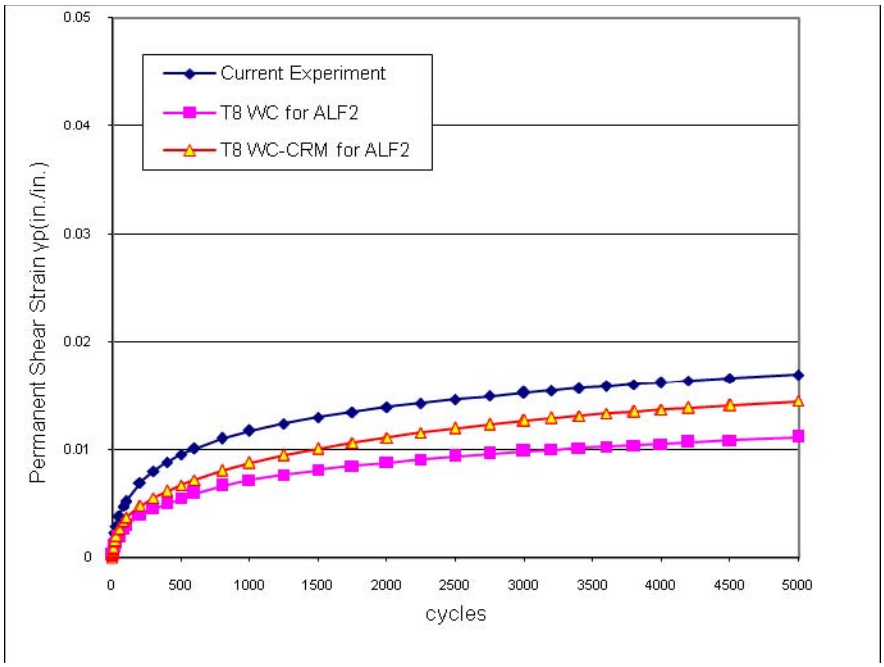

Figure 18
Comparison of permanent strain for the mixtures used in ALF 2 and 3

Table 19
Resilient Modulus of Crushed Stone and RAP Material

Resilient Modulus Mr (ksi /MPa)							
Sample ID	1	2	3	4	Ave.	STD	CV%
Crushed Stone	29 (197)	31 (213)	29 (201)	28 (190)	29.04 (200.25)	1.26 (9.64)	4.814
RAP	26 (180)	35 (238)	43 (298)	36 (247)	34.91 (240.75)	6.97 (48.35)	20.09
T-test	P-value		0.1515				
	Conclusion		Non-significant difference				

Field Experimental Results

Field experiments included the measurements of rutting and nondestructive testing (Dynaflect and FWD) as well as density. Field measurements were obtained through A-Frame, Dynaflect, FWD, PQI and pressure cells and strain gauges instrumented in the tested pavements. Each measurement was tested for several times at different stations, and the average was considered the representative value for the tested lane.

Measurements of Rutting

Field rutting was measured after every 25,000 ALF load applications. For each test lane, the measurements were taken at eight stations over a length of 30' (9.14m) within the 40' (12.19m) loading length.

Figure 19 depicts the average rut depth development with loading for all three tested lanes. It shows that Lane 1, with RAP interlay on 10" cement treated soil, performed best among the three test lanes in terms of permanent deformation because the rut depth value and rut development rate of Lane 1 are the lowest of the three. Lanes 2 and 3 experience a similar rutting progress. It should be pointed out here that after 1.2 million ESALs loading, some local failures (e.g. potholes) were observed in Lane 2. After careful field investigation, those local failures were identified to be limited only within the surface asphalt mixtures. As this study was mainly about the performance of base course materials and the surface failure could be due to construction variation, a decision was made to patch those failure areas, and the ALF loading was resumed after patching. A slight decrease in the average rut depth measurements for Lane 2 after 1.2 million ESALs was due to surface patching.

To further analyze the rutting data, the variation in rut depth measurements is considered in this study. Figure 20 presents the average rut depth as well as the calculated variation in rut depth versus load of lanes 1 and 2. With the average rut depth and standard deviation, the upper limit (UL) and lower limit (LL) of a 95 percent confidence level are established at each measuring load cycle with equations 10 and 11 based on a t-test. Similarly, Figure 21 compares the rut depth of lanes 2 and 3. It shows that at 95 percent confidence, the rut depth of Lane 1 was significantly smaller than Lane 2 and Lane 3 (with little overlap of Lane 1 with lanes 2 and 3 at the end of the loading period), while the rut depths of Lane 2 and Lane 3 are similar (as the majority of the hatched areas were overlapped). This observation proves the results of average rut depth shown in Figure 19.

$$UL = d_{ave} + t_{\alpha/2} * s/n^{1/2} \quad (10)$$

$$LL = d_{ave} - t_{\alpha/2} * s/n^{1/2} \quad (11)$$

where,

UL = upper limit of rut depth, inch;

LL = lower limit of rut depth, inch;

d_{ave}= average rut depth, inch;

$t_{\alpha/2}$ = t value at confidence level of 95%;

s = standard deviation; and

n = measuring sample number.

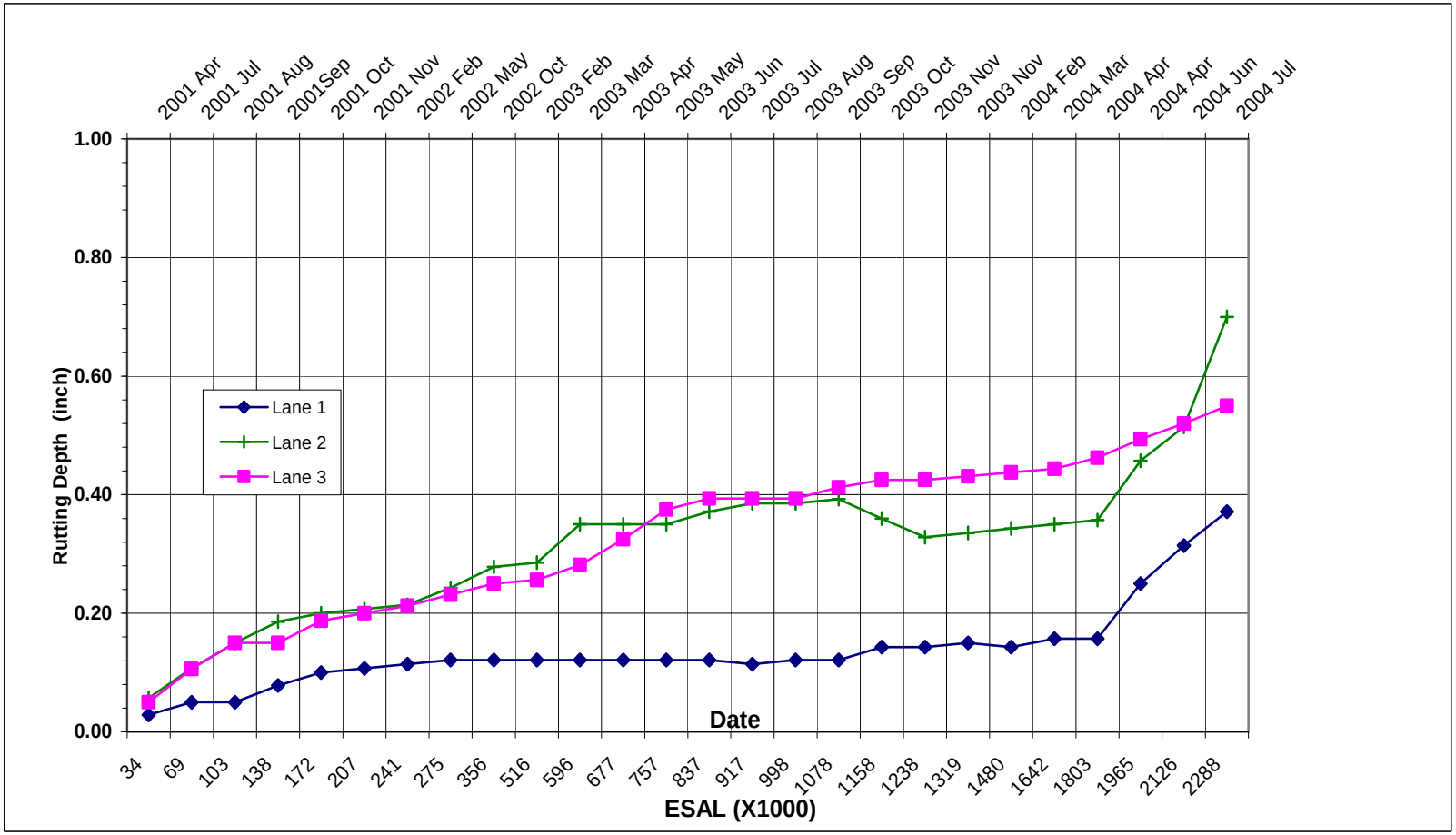

Figure 19
Average rut depth

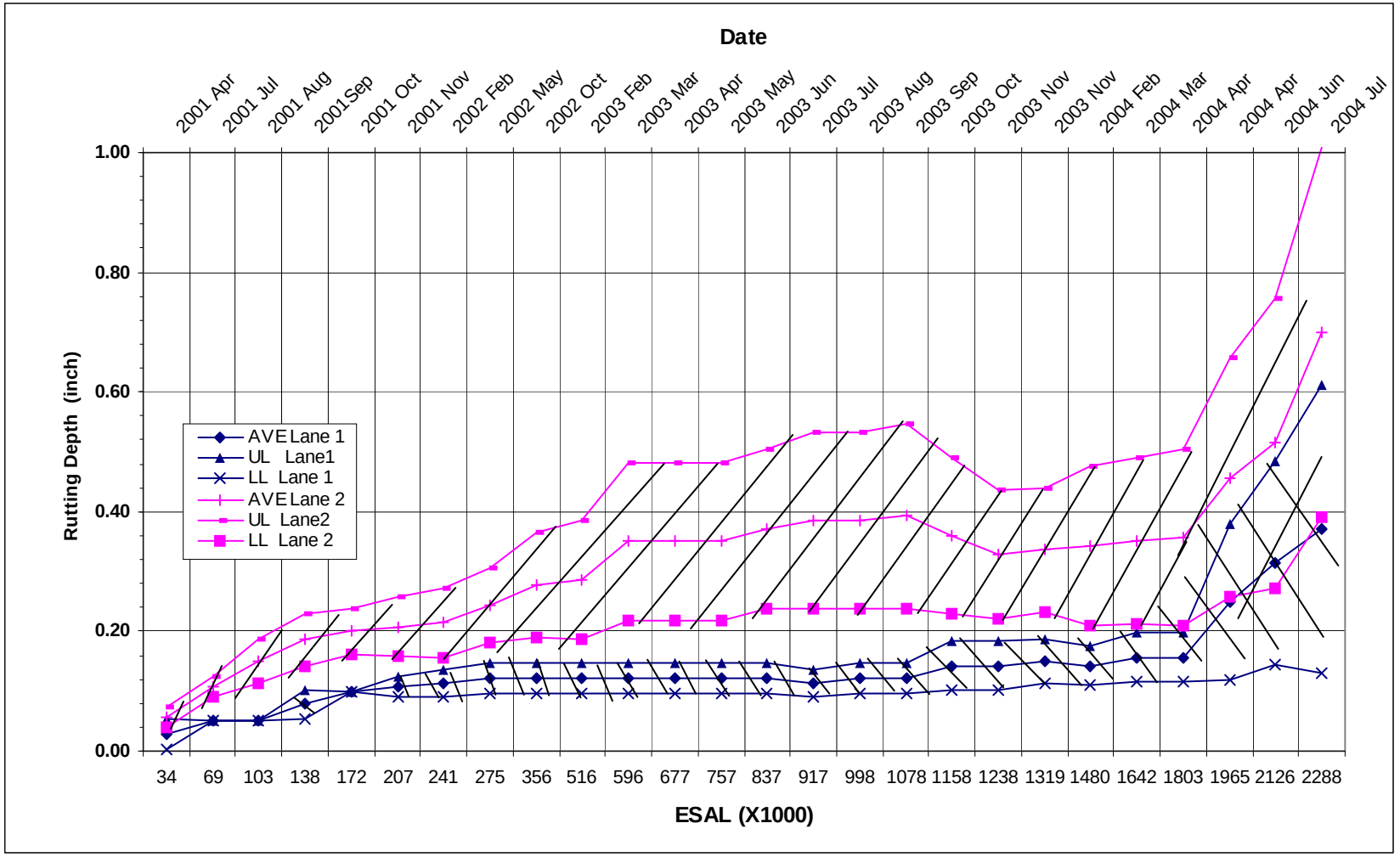

Figure 20
Rutting depth for lanes 1 and 2 with 95% confidence

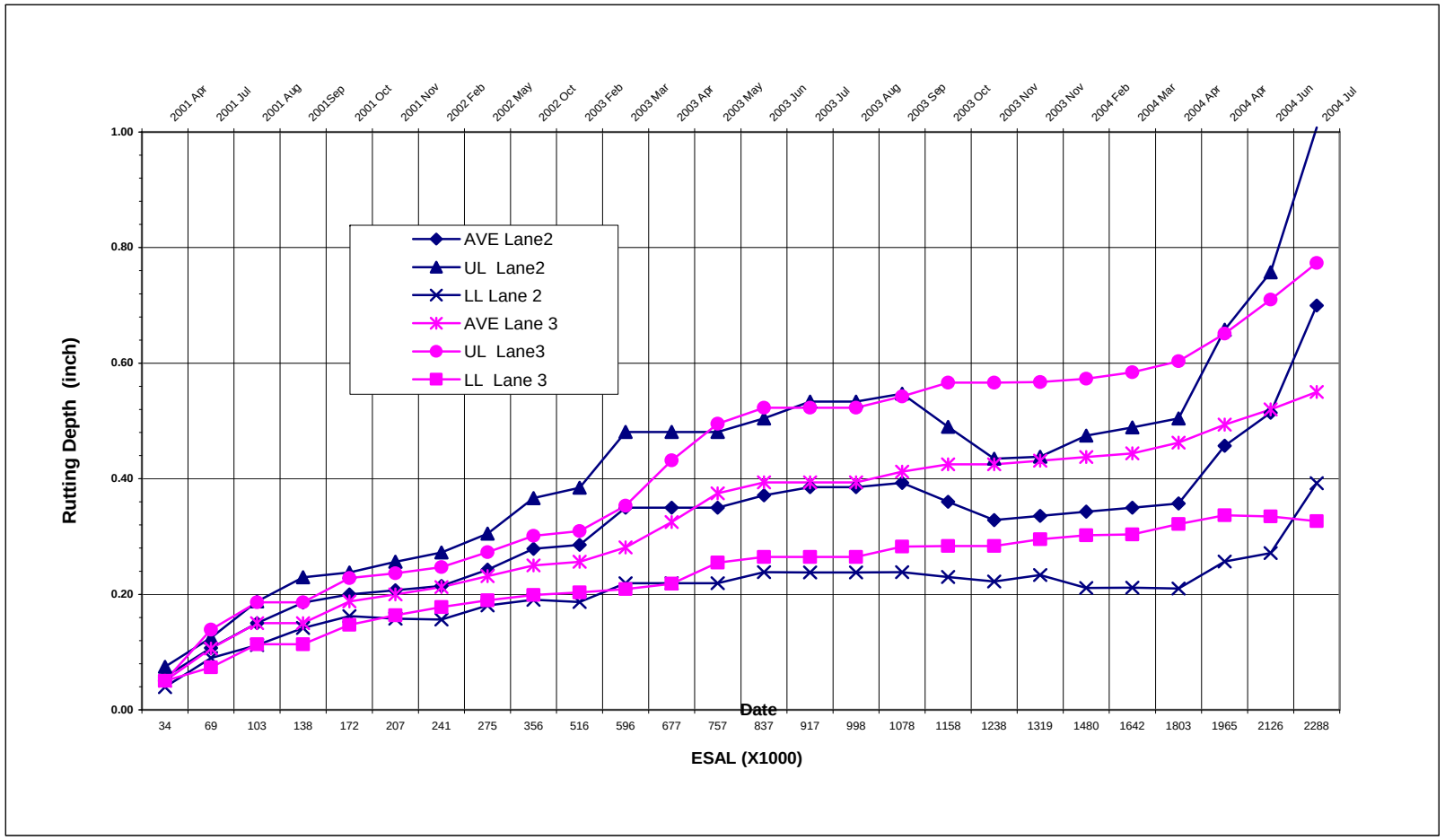

Figure 21
Rutting depth for lanes 2 and 3 with 95% confidence

Dynaflect Measurement

The primary data obtained from the Dynaflect test are 5 geophone deflections. After being adjusted to a standard temperature of 60°F, the Dynaflect deflection can be used to calculate the Structural Number (SN) of the test pavement. With the subgrade modulus (Es) - SN relationship, the subgrade modulus of test pavement can be calculated. Therefore, the following discussion will focus on the SN and Es obtained from the Dynaflect test.

Dynaflect Structural Number (SN). Figure 22 presents the average Dynaflect SN of three test lanes versus ESAL. Lane 1, with RAP interlay on a 10" cement treated soil layer, possesses the highest SN among the three tested lanes, with a value of 4.9 at the beginning and 3.8 after 2,288E+4 ESAL loading. Lane 2 and Lane 3 have similar SN during the whole loading period. These results are consistent with the observation of rutting measurements discussed above, which show that RAP and stone are structurally similar in the pavement layer, and the thicker cement treated layer (10") performs significantly better than thinner (6") cement stabilized layer.

Dynaflect Subgrade Modulus. Figure 23 shows a typical relation between rain fall amounts and the E_s values during the loading period. It is noted that rainfall data did not present significant impact on the variation of the subgrade modulus, indicating that the drainage system installed was effective in eliminating the impact of the moisture in the foundation layers.

Figure 24 presents the seasonal variation of the subgrade modulus of three different lanes obtained from Dynaflect test. It shows that the subgrade modulus (E_s) of the three lanes had similar trends during the whole loading period.

FWD Measurement

The following discussion covers the analysis of the modulus of each layer of test pavement. Based on this, the influence of temperature and loading on surface AC layer modulus, the relationship between FWD backcalculated subgrade modulus and Dynafelct subgrade modulus are studied. Furthermore, the relationship between FWD backcalculated subgrade modulus and FWD deflection d7 are analyzed as well.

FWD Backcalculated Modulus of Surface AC. To show the influence of temperature on surface AC modulus, the moduli and pavement temperature measured with FWD are presented in figure 25. It shows a moderate line correlation between the AC moduli and pavement temperature; with the increase of temperature, the AC modulus decreases accordingly.

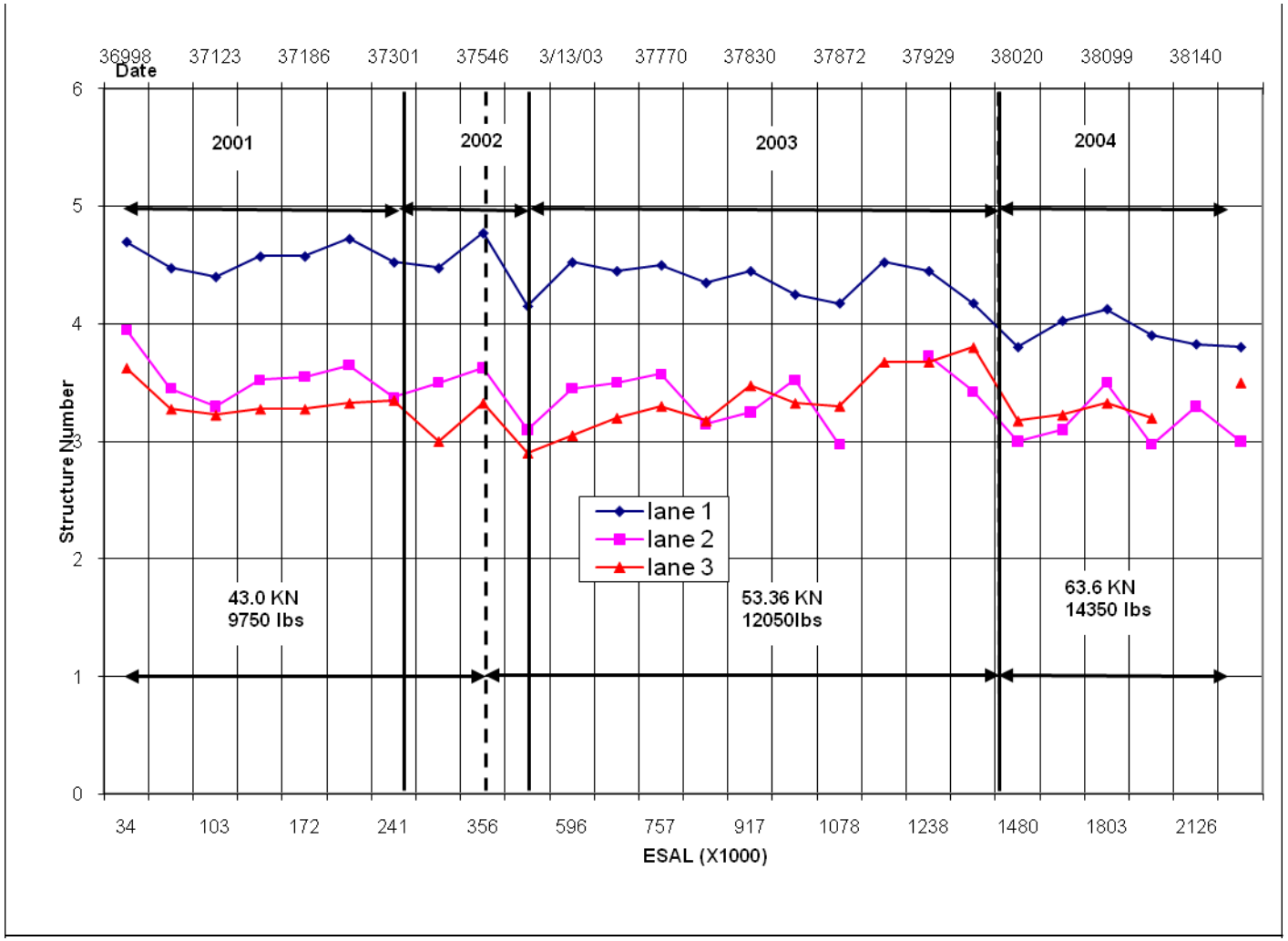

Figure 22
Dynaflect structure number

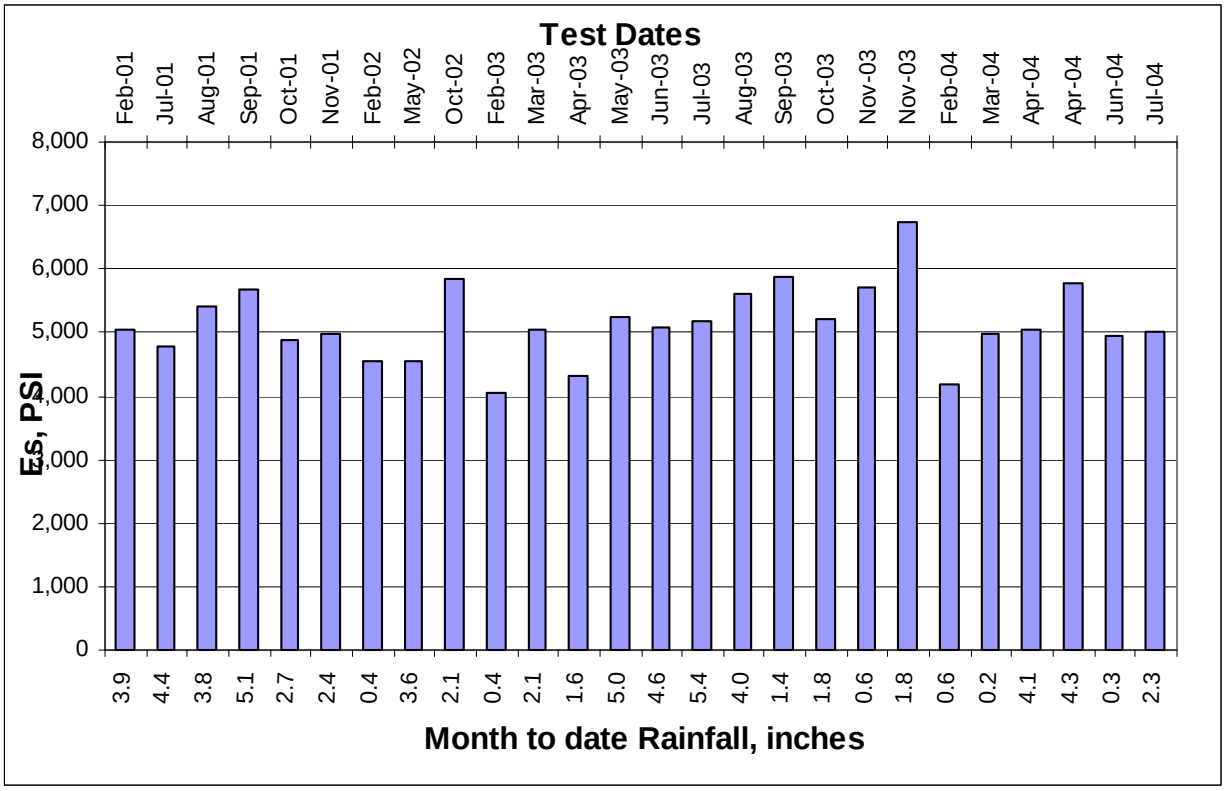

Figure 23
Subgrade modulus versus rainfall for lane 1

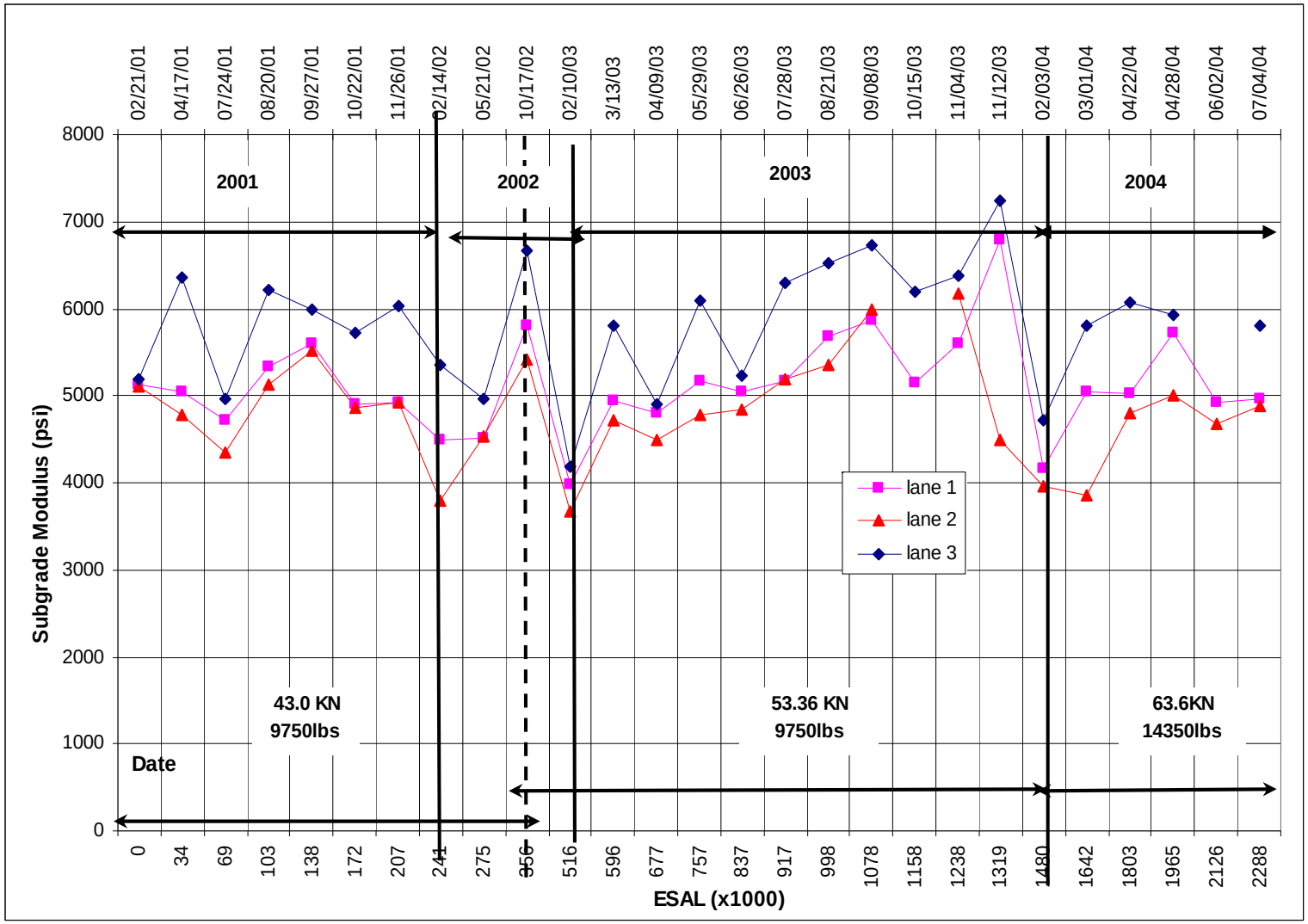

Figure 24
Dynaflect subgrade modulus

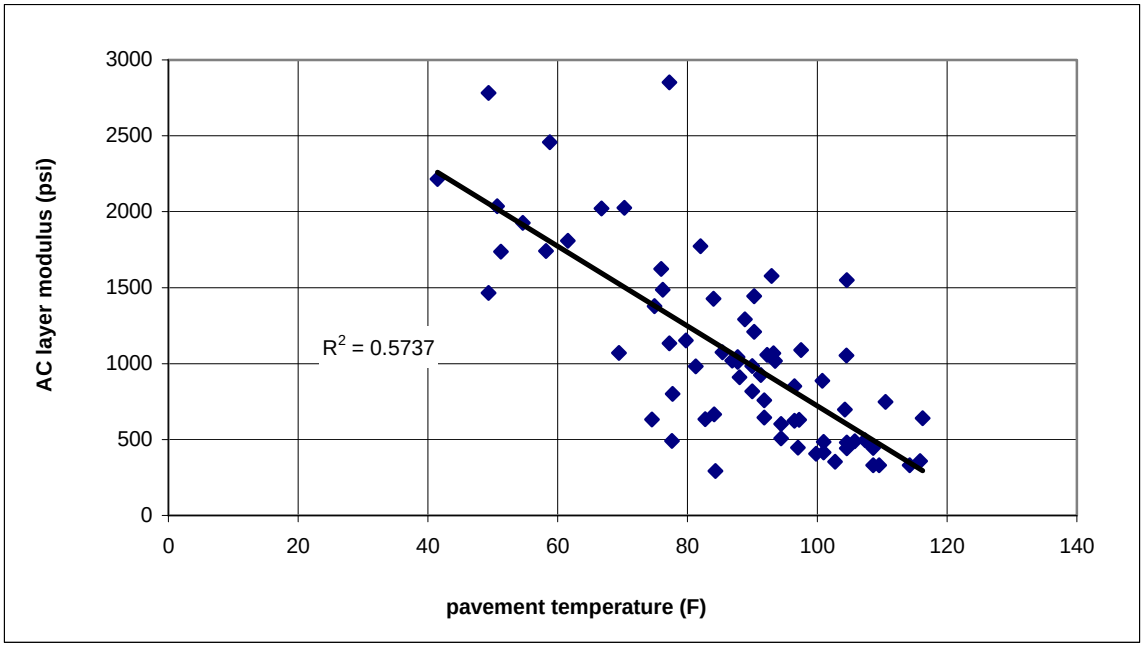

Figure 25
Relationship between modulus of surface AC and pavement temperature

In order to analyze the influence of load on surface AC moduli and pavement structure capacity, one temperature interval (91ºF-114º F) is selected, and FWD backcalculated AC modulus as well as FWD deflection d1 versus ESALS figures for all three lanes are drawn (figures 26, 27).

A good correlation is observed between FWD backcalculated AC modulus and sensor d1 deflection with ESALs, as shown in figures 26 and 27, respectively. They show that the AC modulus decreases with the loading at the fixed temperature interval, while d1 increases with the loading. This indicates that besides temperature, accelerated loading is another key factor to affect the AC modulus, and with the accumulated loading, the AC layer deteriorates. Furthermore, it is noted that with same AC layer, Lane 1 possesses the lower d1 value compared to lanes 2 and 3, which is consistent with the results of rut depth. This observation shows that AC modulus is not the main reason for rutting. To draw a clear relationship between AC modulus and ESALs, Figure 28 depicts the modulus data of all three lanes together, with one single regression line with R^2= 0.63.

Figure 29 presents the average normal backcalculated modulus of surface AC of three test lanes. The data presented indicate the general variation in modulus value, which shows higher values in the cold period and lower values in the warm period.

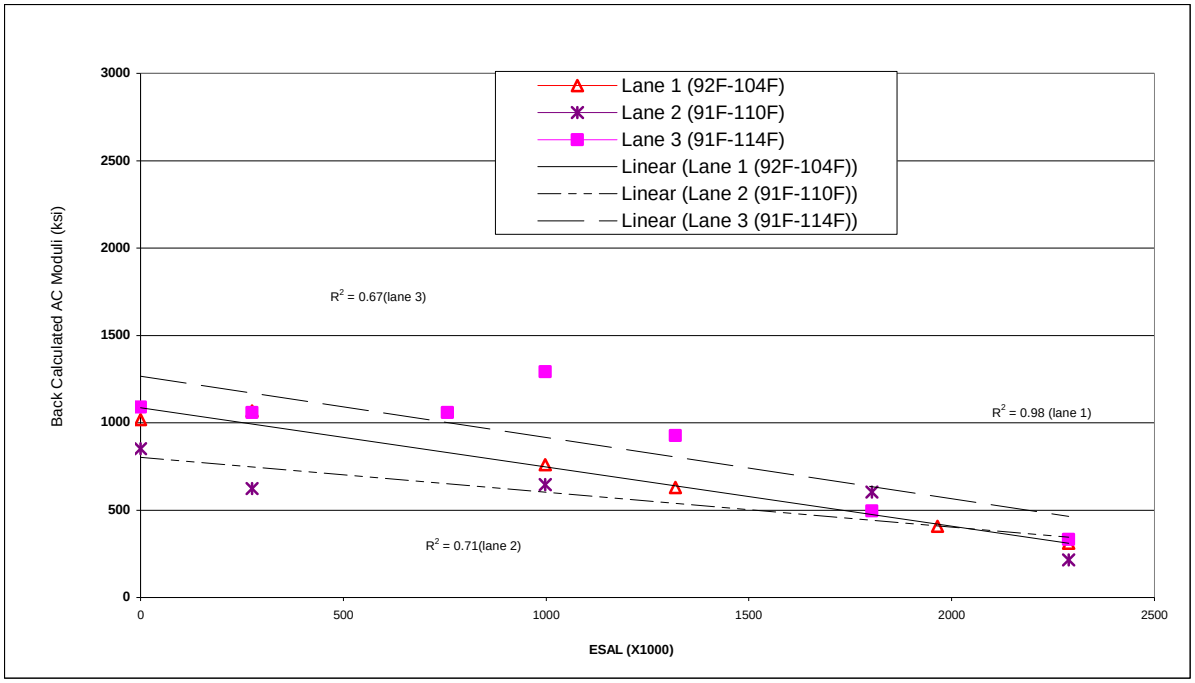

Figure 26
Modulus of surface AC versus ESALs (91F-114F)

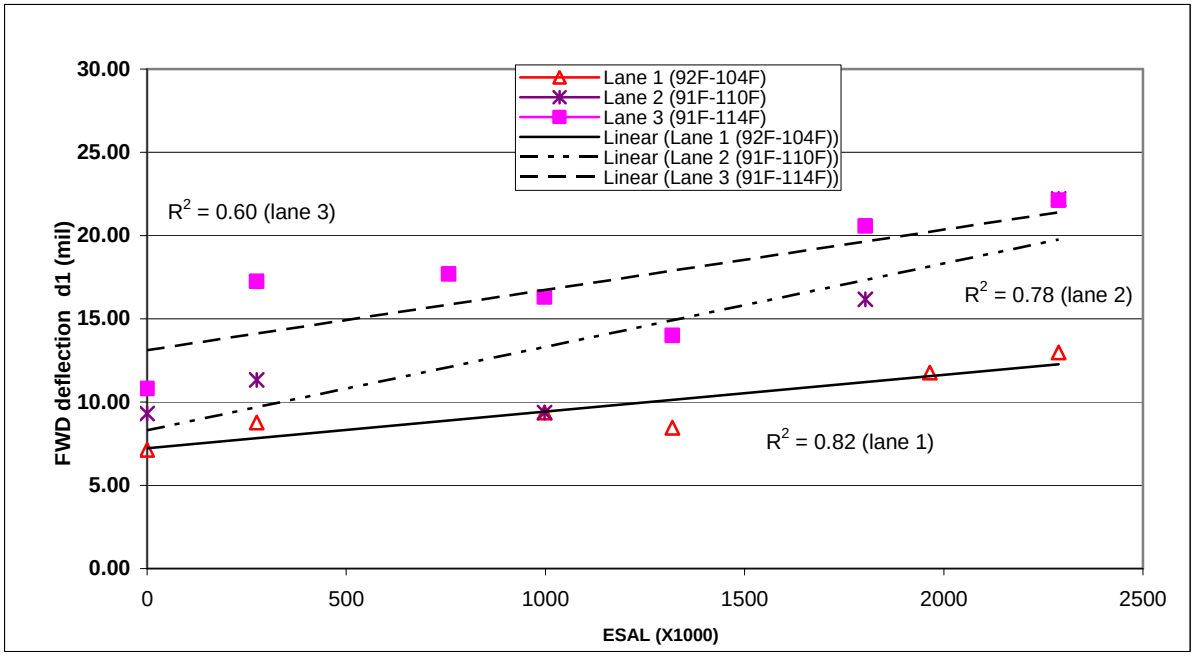

Figure 27
FWD deflection d1 versus ESALs (91F-114F)

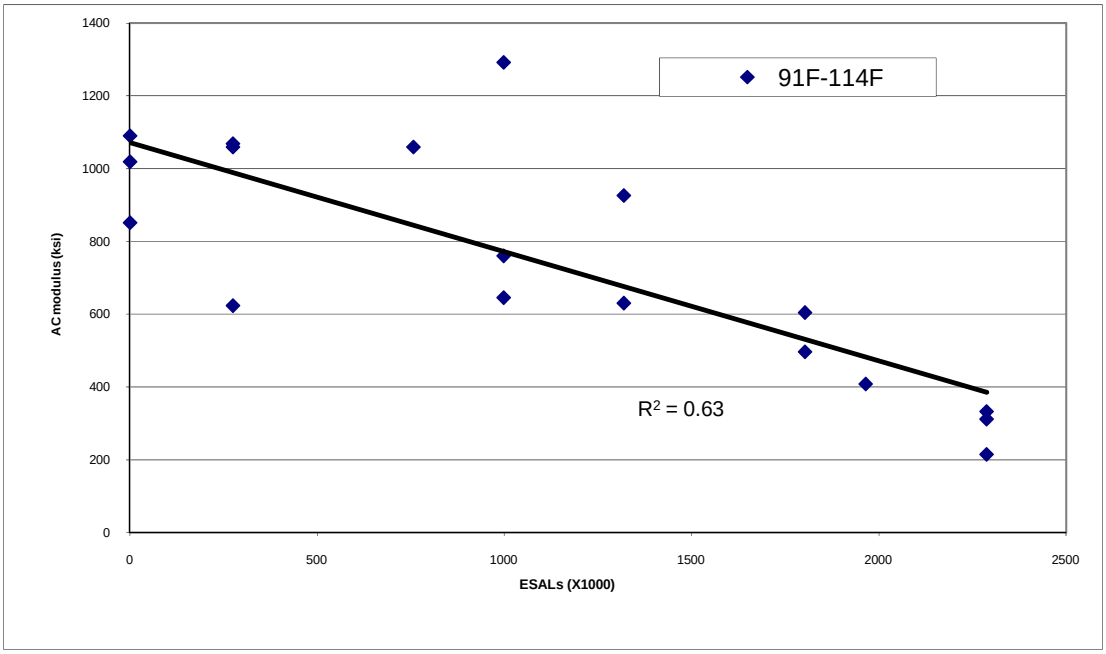

Figure 28
Modulus of surface AC versus ESALs for all three lanes (91F-114F)

FWD Backcalculated Modulus of Interlayer. Figure 30 shows the average back calculated moduli of the interlayers. The fluctuation of data can also be explained with the change in test temperature. It is noted that the interlayer modulus of Lane 3 shows less temperature susceptibility than lanes 1 and 2, as Lane 3 does not contain RAP material. Comparing the modulus value of 34E+3 ESAL to that of 1,803E+3ESAL (both are tested during spring), it is clear that the interlayer modulus of each of the three pavements decreases with accelerated loading.

FWD Backcalculated Modulus of Soil Cement. Figure 31 shows the average backcalculated modulus of the soil cement layers of the three tested pavement structures. It shows that throughout the loading procedure, the backcalculated subbase modulus of Lane 1 is higher than that of lanes 2 and 3, while the values of lanes 2 and 3 are similar.

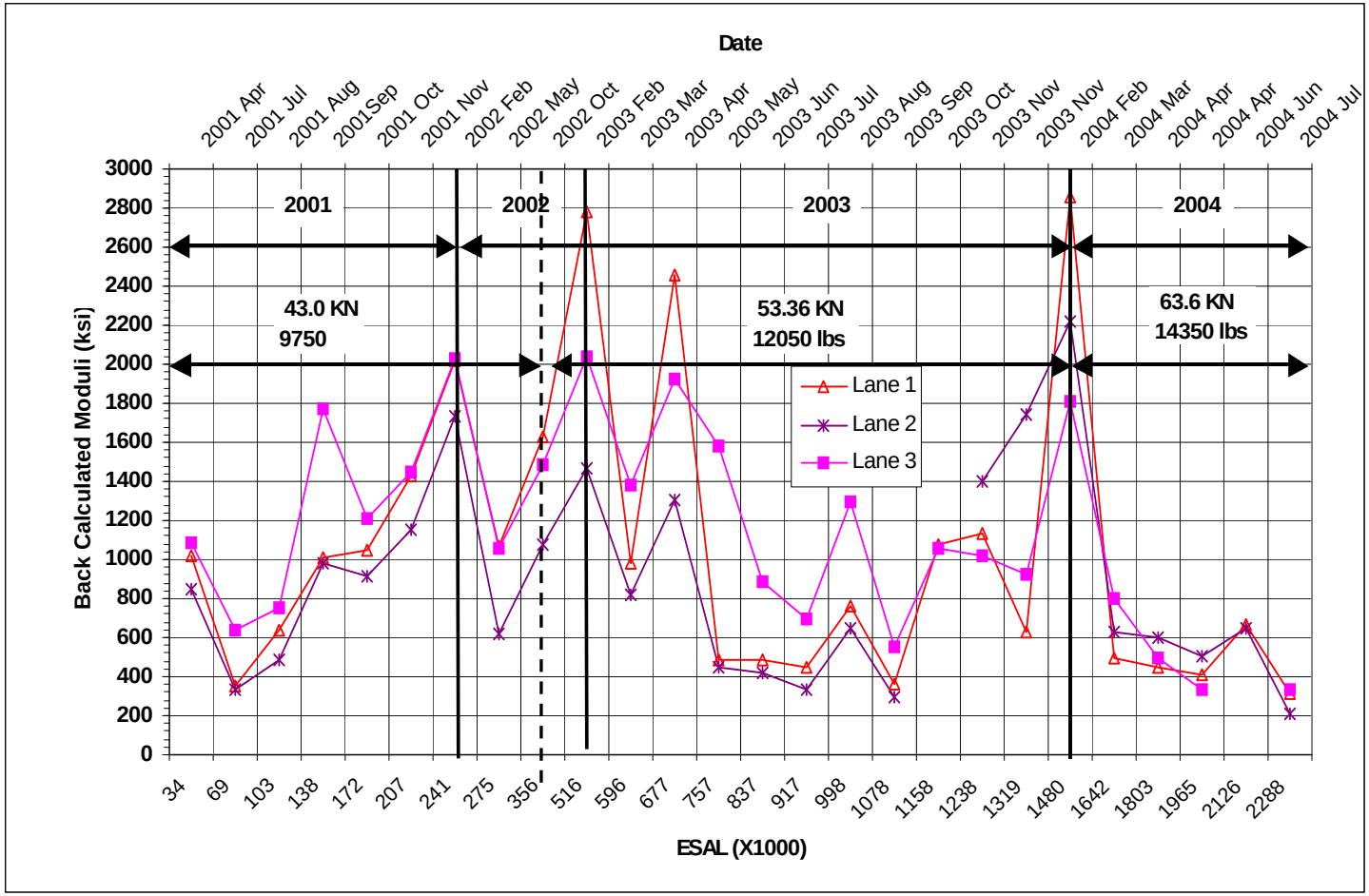

Figure 29
FWD backcalculated modulus of surface AC

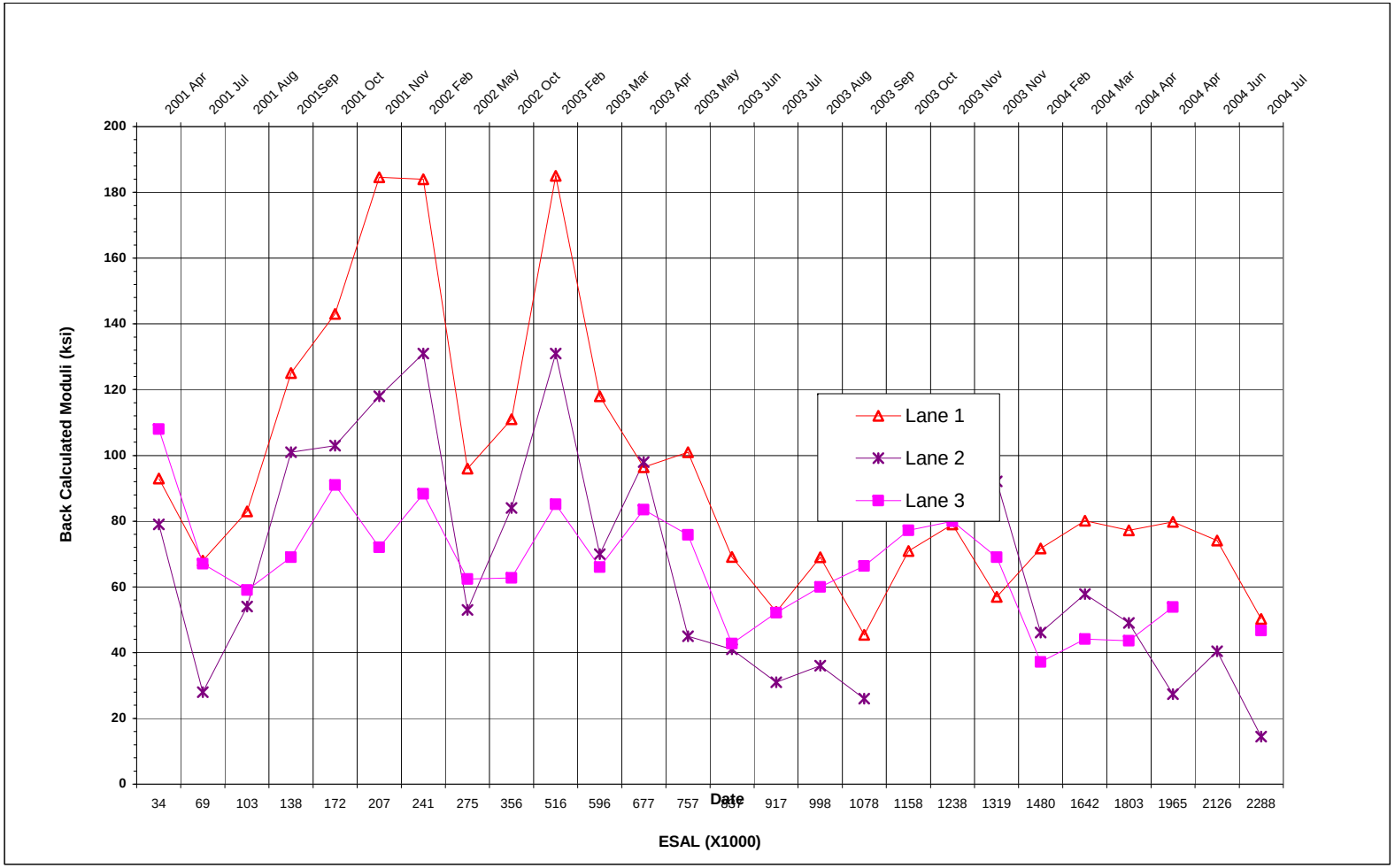

Figure 30
FWD backcalculated modulus of interlayer

This result is not consistent with the physical property of the subgrade material. It is known that the soil cement with higher cement content possesses higher modulus, but the backcalculated modulus give the opposite results. That is, Lane 1, with 10" 5 percent content cement treated soil, exhibits higher modulus than Lane 2 and Lane 3 with 6" 10 percent content cement stabilized soil. The reason lies in the backcalculation employed in the Elmod 5 software package. In this project, the Deflection Basin Fit method is used to calculate the modulus of each layer in the program. The backcalculation procedure is as follows: First, assume the initial modulus of each layer based on the recommended modulus range. Then Odemark's layer transformation approach is used with Boussinesq's equations to calculate deflection. Next, an iterative procedure is employed to determine if those moduli result in the same deflection as measured. When the RMS (residual mean square) falls into the allowed interval, the iterative procedure is over, and a set of moduli is given. It should be noted that with this method, the backcalculated modulus of each layer is not unique, and it is a multi-solution problem. Concerning the backcalculation of the ALF 3 structure, as the rigidity of the thicker soil cement layer with lower cement content is higher than the thinner layer with high content (which is proved by the rutting data and structure number), it is possible to choose a higher modulus for the thicker soil cement layer and get a set of deflection that fits the measured deflection basin very well. Such does not necessarily mean that the modulus of soil cement with lower cement content is higher than that with higher cement content.

Lane 1 exhibits the lowest rut depth and highest structure number among the three lanes tested. It is noted that the thickness of the soil cement layer also plays an important role in determining its structural capacity in addition to the cement content.

FWD Backcalculated Modulus of Subgrade. In order to analyze the relationship between FWD Backcalculated E_s Modulus and Dynaflect E_s Modulus, a FWD E_s versus Dynaflect E_s figure was drawn in figure 32. No statistical relationship was found between these two moduli values. Figure 33 presents the average FWD back calculated modulus of subgrade of all three lanes.

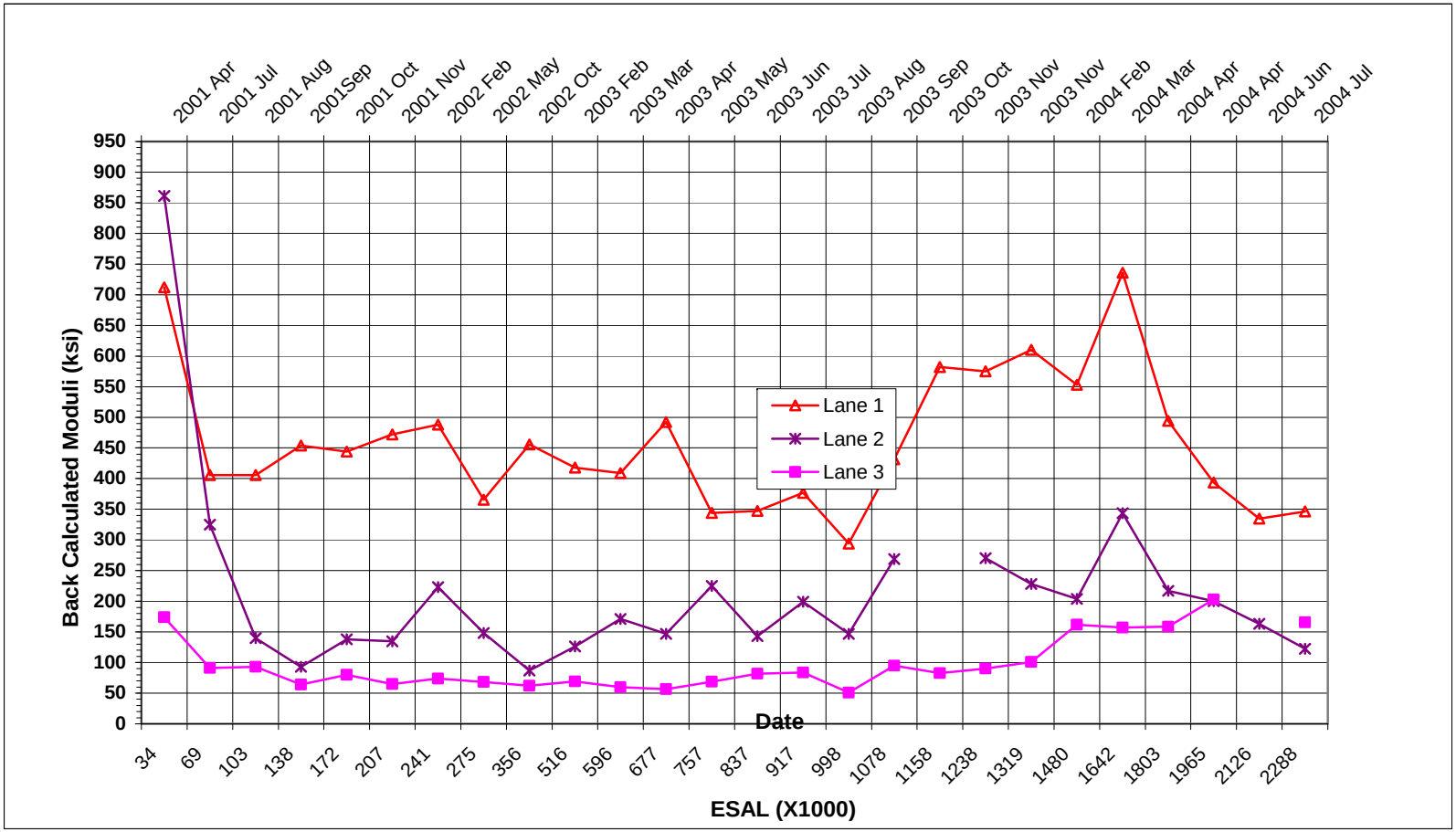

Figure 31
FWD backcalculated modulus of soil cement

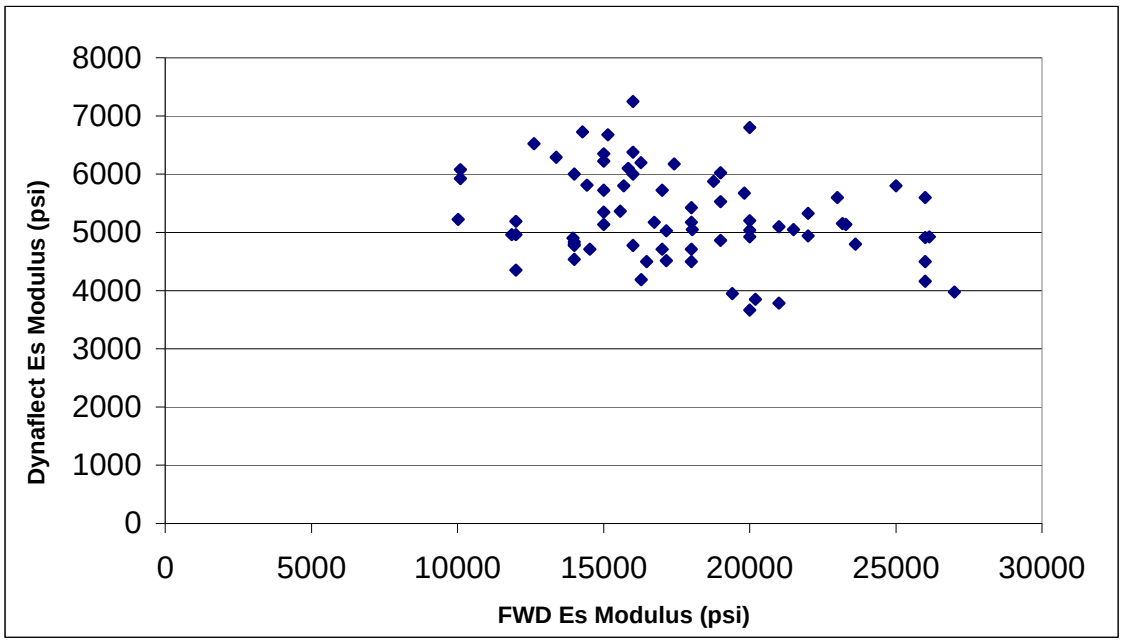

Figure 32
FWD backcalculated E_s modulus versus Dynaflect E_s modulus

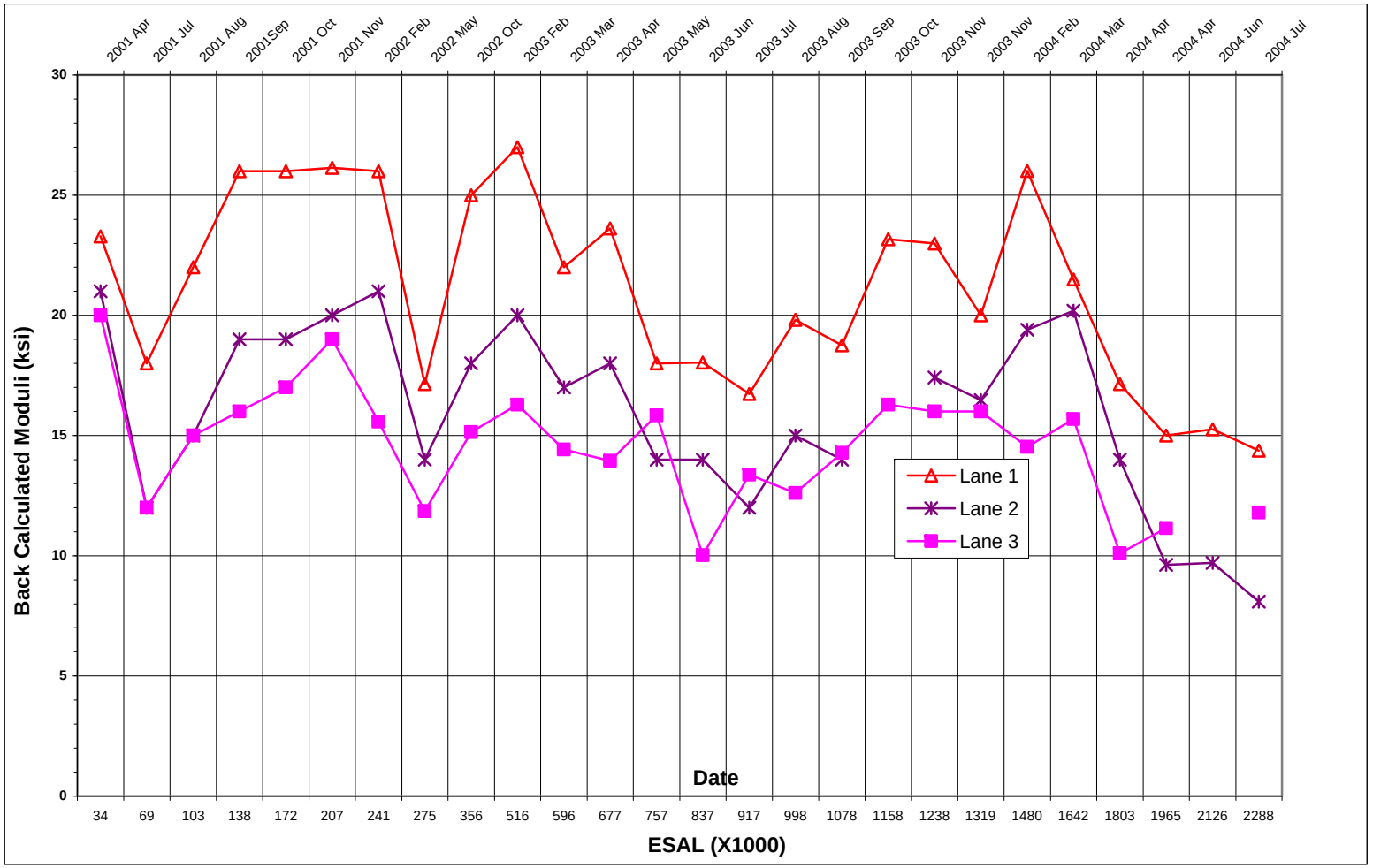

Figure 33
FWD backcalculated modulus of subgrade

Relationship between FWD Subgrade Modulus and Deflection d7. Figure 34 presents the FWD backcalculated modulus values of subgrade layers and the deflection registered by the 7th sensor (d7) of the FWD device for all three tested lanes. Results from the FWD indicate that the subgrade modulus values and d7 data fit very well; that is, when d7 is high, the subgrade modulus value (Es) is low, and vice versa. It was found that the E_s and d7 have a moderate correlated linear relationship with R^2=0.51.

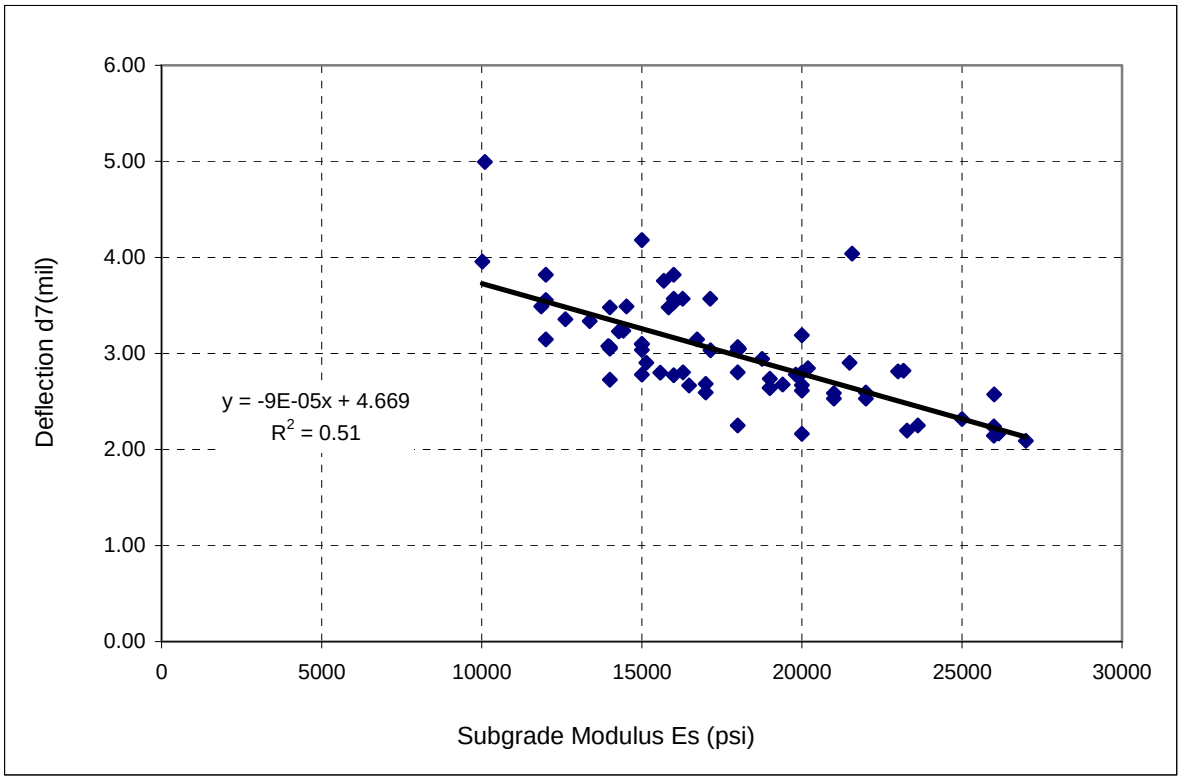

Figure 34
Typical relationship between Es and d7 for lanes 1, 2, and 3

FWD Central Deflection d1. Figure 35 presents the max FWD deflection d1 (first sensor, under the direct impact of FWD load) for all three test lanes. At the beginning (0 load repetition), all three lanes showed small surface deflections. As the ALF load repetitions continuously increased, pavement materials started to deteriorate and the capacities of pavement structures decreased. This is evidenced by the increased FWD surface deflections for all three lanes. Interestingly, Lane 1 with RAP interlayer on 10" cement treated soil layer possesses the lowest deflection among the three tested lanes, which indicates the highest pavement structure capacity. The deflections of Lane 2 and Lane 3 are similar during the loading period. These measurements are consistent with the observation of rut depth and Dynaflect SN results discussed above, and they show that RAP and stone base could have

compatible pavement performance and the thicker cement treated layer is structurally stronger than thinner cement stabilized layer.

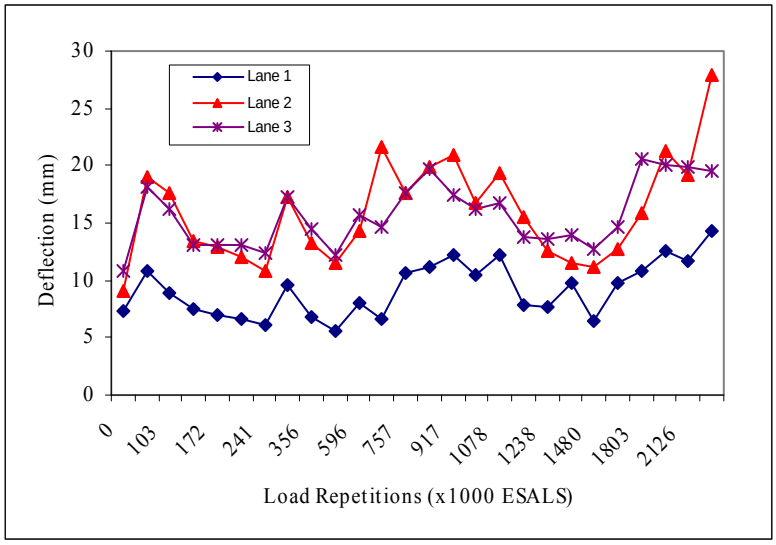

Figure 35
FWD central deflection d1

Pavement Quality Indicator (PQI) Density of Asphalt Cement Layer
The following discussion includes the analysis of PQI density data of asphalt cement layer and the relationship between PQI density and rut depth for all three tested lanes.

PQI Density Measurements. Figure 36 presents the average PQI density for lanes 1, 2 and 3. Despite the fluctuation, the density values do not change significantly during the first 917,000 ESALs, and they experience a slight increase in the next loading period from 917,000 to 1,642,000 ESAL. At the end of experiment, the density increases significantly. It should be noted that the density decreases somehow at the beginning and the end of the experiment, which is against the densification phenomena and shows that PQI is not sensitive to pavement densification.

Relationship between Density and Rut Depth
Figure 37 presents the density and rut depth measured during the loading period for lanes 1, 2, and 3. As shown in the figure, no corresponding relationship was found between density and rut depth. Furthermore, no statistical relationship is observed between the density and rut depth based on the data obtained from this experiment.

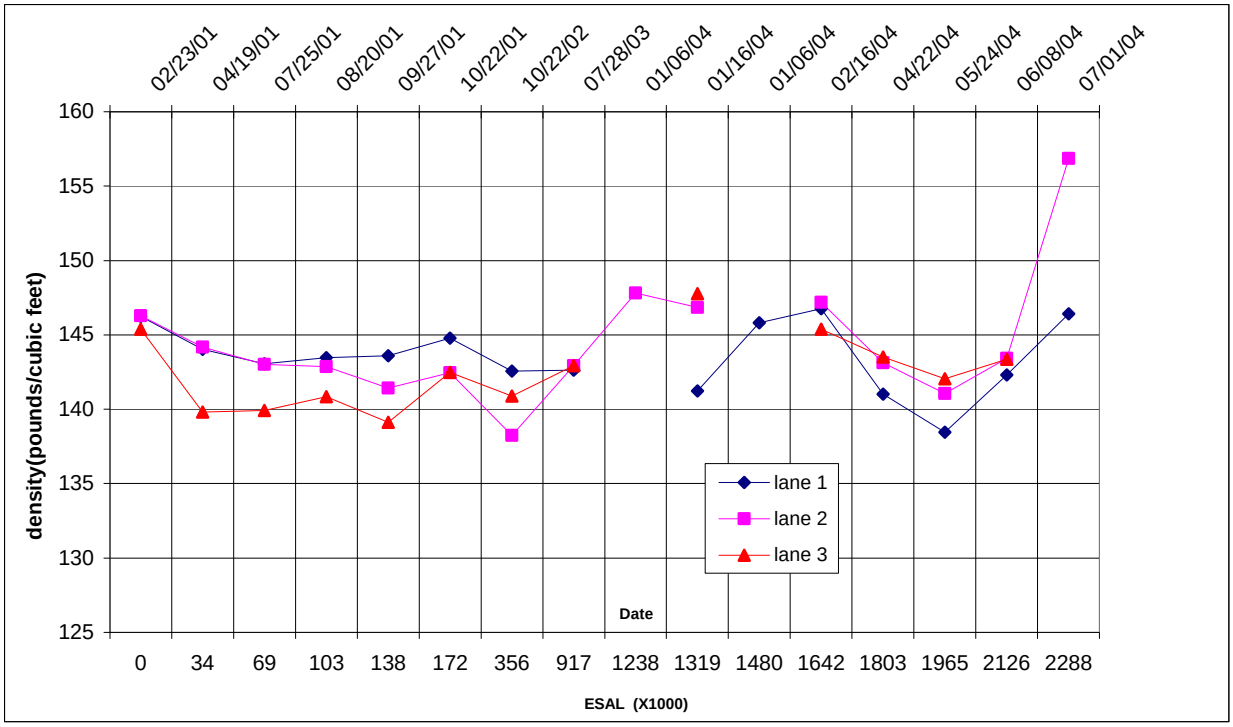

Figure 36
PQI density measurements for lanes 1, 2, and 3

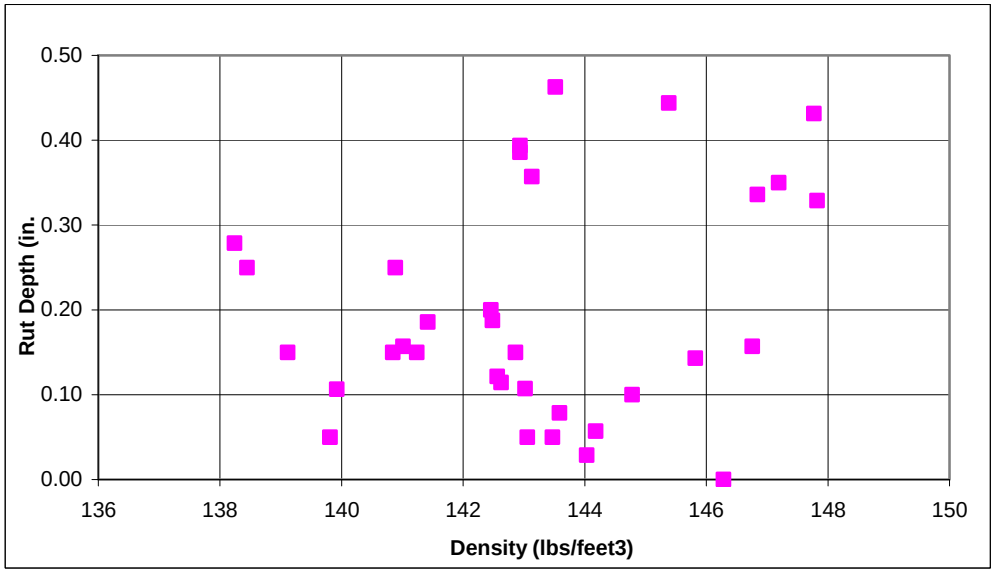

Figure 37
Density versus rut depth for all three lanes

Life Cycle Cost of Stone and RAP Interlayer

Table 20 shows the life cycle cost of high volume stone interlayer and high volume RAP interlayer. It indicates that RAP interlayer is more cost effective than stone interlayer in terms of initial cost and life cycle cost.

Table 20

Life Cycle Cost of Stone and RAP Interlayer

Pavement Type	High Volume Stone Interlayer	High Volume RAP Interlayer
Initial cost/ yd^2, 4 " stone or RAP over 8.5" of stabilized soil	$8.4	$5.28 Assuming zero cost for RAP
Asphalt Cost	$41.7/ton	$41.7/ton
Cost Lane Mile, Base Course	$59,136	$37.171
Cost Lane Mile AC, 9"	$151,921	$151,921
Total Pavement (AC+ Base)	$211,057	$189,092
Life from ALF (ESALs), project to failure at 3/4" rut	>3 million ESALs	>3 million ESALs
Life performance Ratio, Actual from ALF	1	1
Estimated Field Life Ratio	1	1
Maintenance cost assuming a 30 year design	Mill 2 " replace 3.5 " $66,965	Mill 2 " replace 3.5 " $66,965
PW cost of initial and future maintenance	$278,022	$256,057
Life cycle cost/lane-mile/year, using uniform annualized series	$16,078	$14,808

CONCLUSIONS

A comprehensive study was conducted to evaluate the appropriateness of using recycled or reclaimed asphalt pavement as an alternative to crushed stone interlayer in base course through laboratory characterization and field experiments. In addition, the performance of soil cement was investigated by varying layer thickness and cement content. The resilient moduli of RAP and crushed stone were examined in the laboratory. Three test lanes were constructed and subjected to accelerated loading at the Louisiana Pavement Research Facility (LPRF). The rut depth, Dynaflect, FWD deflections, and density were measured periodically for each test lane.

Laboratory and field test results indicate that the performance of RAP and crushed stone are similar when used as a base course over a cement stabilized layer. This study also confirmed the results from the first ALF experiments, which showed that a stronger layer was achieved when a thicker layer of cement treated soil was utilized. Therefore, another primary conclusion drawn from this study is that the thickness of soil cement also plays an important role in determining its capacity, along with the cement content. The following are specific observations drawn from the test results:

- The statistical t-test results indicate that there is no significant difference between resilient modulus of RAP and crushed stone measured in the laboratory.
- ALF test results indicate the rut depth of Lane 1 was significantly lower than that of Lane 2 and Lane 3, and the rut development on Lane 2 was similar to that of Lane 3.
- Based on the Dynaflect SN results, Lane 1 was structurally stronger than that of Lane 2 and Lane 3, and both Lane 2 and Lane 3 were observed to have similar structure capacity.
- Rainfall data had little impact on the variation of the subgrade modulus, indicating that the drainage system installed was effective in eliminating the impact of the moisture in the foundation layers
- Based on the FWD test results, Lane 1 exhibited lower d_1 deflection than Lane 2 and Lane 3, whereas Lane 1 and Lane 2 exhibited similar d_1 deflection.
- The FWD backcalculated base course modulus results show that untreated RAP and stone base have similar modulus.

- A good correlation was observed between FWD backcalculated AC modulus with pavement temperature and load repetitions; AC modulus decreased with an increase in pavement temperature and accumulation of ESLAs.
- A good linear relationship was observed between FWD backcalculated subgrade modulus and FWD deflection d7.
- PQI density measurements were sensitive to pavement densification.
- No statistical relationship was observed between density and rut depth.
- Life cycle cost analysis shows that the RAP interlayer is more cost effective than the stone interlayer.

RECOMMENDATIONS

RAP is recommended for use as an interlayer base course over cement stabilized or cement treated layers for construction of the flexible pavements.

The present research was limited to the loading capacity of the pavement structure due to the nature of accelerated loading. Future research should be carried out to investigate the long-term influence of environmental conditions on the performance of pavement containing RAP interlayer. Also, additional laboratory analysis on the compactive efforts of RAP would be beneficial in developing specifications for the use of RAP as a raw base material.

REFERENCES

1. King, W.M. Jr., *Evaluation of Stone/RAP Interlay Under Accelerated Loading, (Construction Report*), Louisiana Transportation Research Center, 2001.

2. Mohammad, L.N., and Paul, H.R., *Evaluation of the Indirect Tensile Test for Determining the Structural Properties of Asphalt Mix,* Transportation Research Record 1417, Transportation Research Board, Washington, D.C., 1993, pp. 58-63.

3. TxDOT, *Test Method Tex-321-F,* Texas Department of Transportation, Division of Materials And Tests, Austin, TX, Revised February, 1993

4. Mohammad, L.N., Zhang, X., Huang, B., and Tan, Z., *Laboratory Performance Evaluation of SMA, CMHB, and Dense Graded Asphalt Mixtures,* Journal of the Asphalt Paving Technologists, Vol. 68, 1999, pp. 252-283.

5. Sousa, J., Solaimanian, M., and Weissman, *Development and Use of the Repeated Shear Test (Constant Height): An Optional Mix Design Tool*, SHRP-A-698, Strategic Highway Research Program, National Research Council, Washington, D.C., 1994.

6. Louisiana DOTD, *Louisiana Standard Specifications for Roads and Bridges,* Louisiana Department of Transportation and Development, Baton Rouge, LA, 2000.

7. American Association of State and Highway Transportation Officials, *Standard Specifications for Transportation Materials and Methods of Sampling and Testing,* 23rd Edition, 2003.

8. Mohammad, L. and Wu, Z. "*Sensitivity of Mixture Performance Properties to Changes in Asphalt Mixture Type: Case Study*." Proceeding of the Geo-Trans 2004 Conference, the Geo-Institute of the American Society of Civil Engineers (ASCE), Los Angeles, CA, July, 2004.

9. Sousa, J., Solaimanian, M, and Weissman, *Development and Use of the Repeated Shear Test (Constant Height): An Optional Mix Design Tool*, SHRP-A-698, Strategic Highway Research Program, National Research Council, Washington, D.C., 1994.